Leibniz Society of Science at Berlin
Scientific Colloquium
in honour of *Helmut Moritz*
on the occasion of his 80th birthday
Berlin, Germany, 15 November 2013

Boundary Problems of Mathematical Physics in Earth's Gravity Field Studies

Petr Holota

Research Institute of Geodesy, Topography and Cartography
Zdiby, Prague-East, Czech Republic

Preface

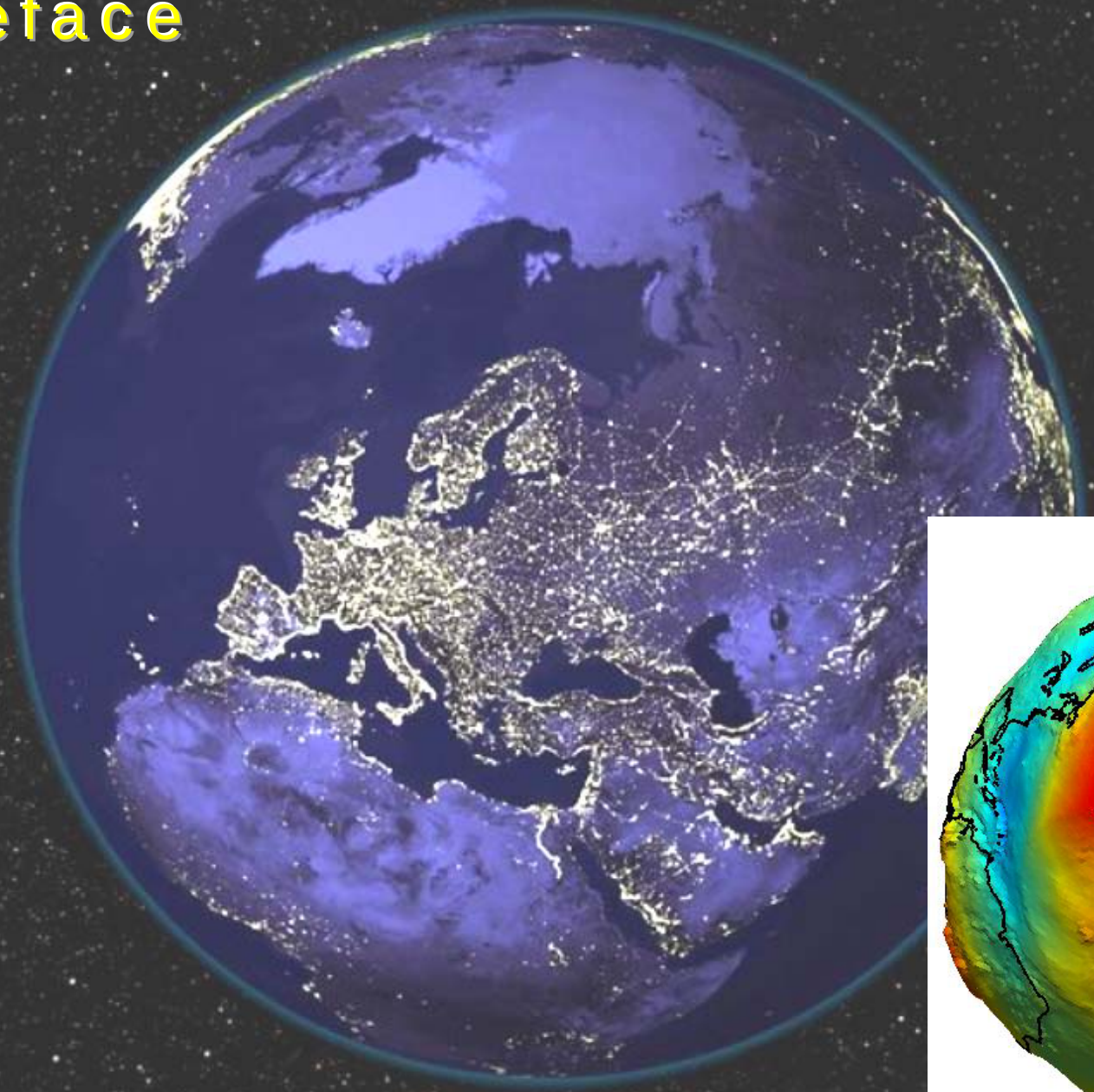

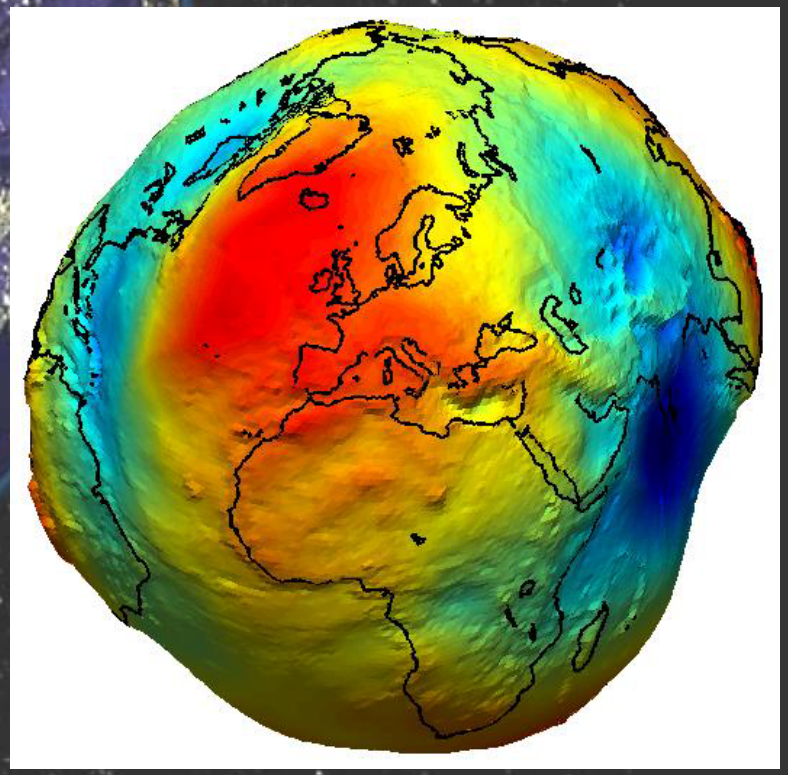

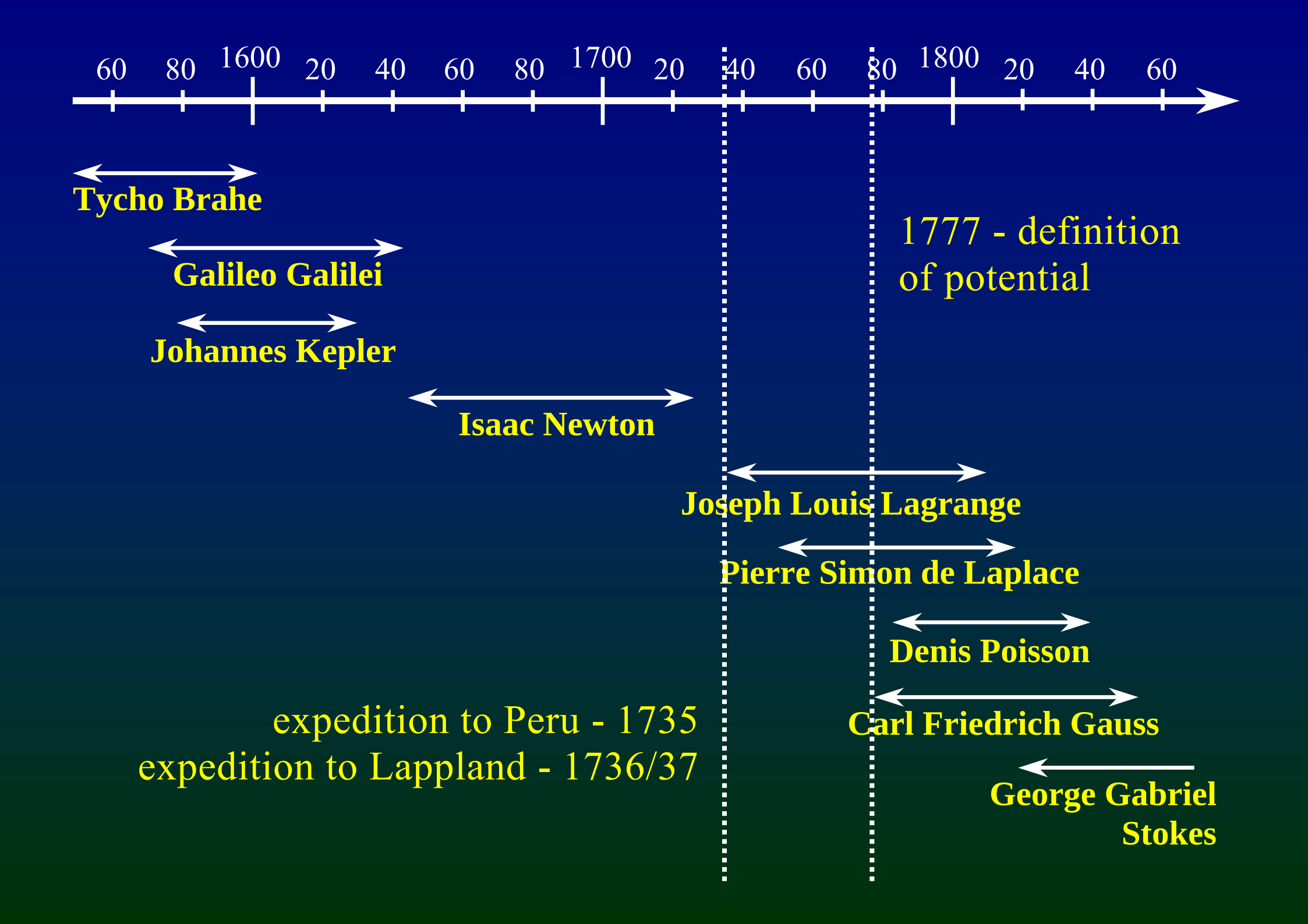
60
80
1600
20
40
60
80
1700
20
40
60
80
1800
20
40
60
Tycho Brahe
Galileo Galilei
Johannes Kepler
Isaac Newton
Joseph Louis Lagrange
Pierre Simon de Laplace
Denis Poisson
Carl Friedrich Gauss
George Gabriel Stokes
1777 - definition of potential
expedition to Peru - 1735
expedition to Lappland - 1736/37

Tycho Brahe (1546 – 1601)

Galileo Galilei (1564 – 1642)

Johannes Kepler (1571 – 1630)

Isaac Newton (1643 – 1727)

Joseph Louis Lagrange (1736 – 1813)

Pierre Simon de Laplace (1749 – 1827)

Denis Poisson (1781 – 1840)

Carl Friedrich Gauss (1777 – 1855)

George Gabriel Stokes (1819 – 1903)

Now we will be more specific

In the determination of the *gravity potential* and *figure* of the Earth from *solely* *terrestrial gravity data* one has to solve a *free boundary-value problem* (which obviously is non-linear) for Laplace's (or Poisson's) equation.

This concept covered several decades of the last century, expressed the *tie between geodesy and mathematics* with an exceptional pregnancy (e.g. *Molodensky*, *Moritz*, *Krarup*, *Hörmander* , but also many others).

Subsequent developments expressed this relation still more distinctly and showed further aspects of the role, the mathematic has in geodesy. This was particularly the case *when satellite data came into play*.

2. Linearized Problem

In practice the approach to the *geodetic free boundary value problem* mostly confines to the solution of its *linearized version*, i.e. to find T such that

$$\Delta T = 0 \qquad \textbf{outside the telluroid}$$

$$T + \langle \boldsymbol{h}, \boldsymbol{grad}\, T \rangle = \Delta W + \langle \boldsymbol{h}, \Delta \boldsymbol{g} \rangle \qquad \textbf{on the telluroid}$$

and that

$$T = \frac{c}{|\boldsymbol{x}|} + O(|\boldsymbol{x}|^{-3}) \qquad \textbf{for} \quad |\boldsymbol{x}| \to \infty$$

where $\boldsymbol{h} = -\boldsymbol{M}^{-1}\boldsymbol{\gamma}$, $\boldsymbol{\gamma} = \boldsymbol{grad}\, U$ **and** $\boldsymbol{M}_{ij} = \dfrac{\partial^2 U}{\partial x_i \partial x_j}$.

The position anomaly is then given by

$$\vec{\zeta} = M^{-1}(\Delta \vec{g} - grad\ T) \ .$$

The following *figure gives the interpretation*.

We suppose that there is a one-to-one correspondence between the points P and Q, e.g. such that

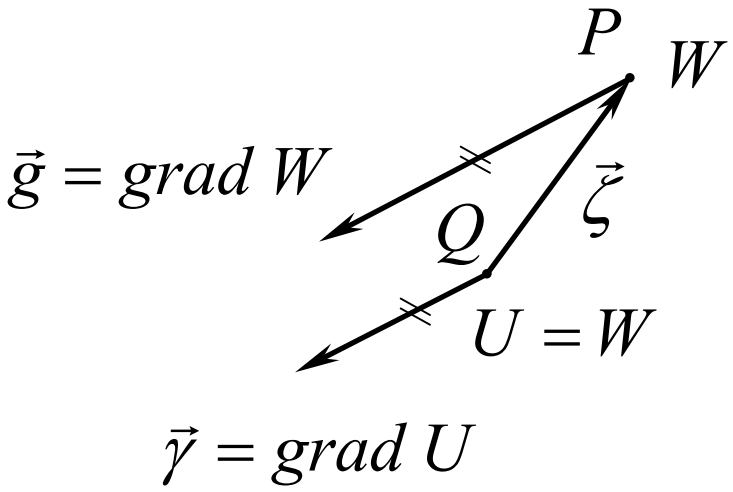

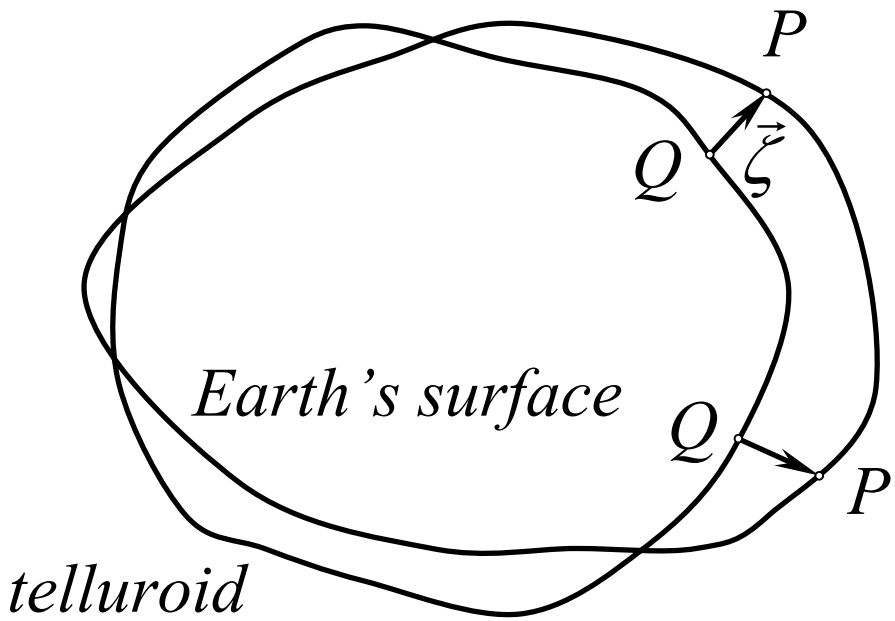

and that the *telluroid* (e.g. *Marussi's telluroid*) represents a model of the Earth's surface .

In addition we suppose that from *geodetic*, *gravimetric* and *astrogeodetic* measurements we know W_P and $\vec{g}_P = grad\ W\big|_P$ on the Earth's surface.

Recall also that in the former practice the boundary problem above was often considerably simplified and treated in the following form

$$\Delta T = 0 \qquad \textbf{for} \quad |\boldsymbol{x}| > R$$

$$R\,\frac{\partial T}{\partial |\boldsymbol{x}|} + 2T = -R\,\Delta g \quad \textbf{for} \quad |\boldsymbol{x}| = R$$

Its solution is given by the famous formula

$$T(\varphi,\lambda) = \frac{R}{4\pi}\int_{\sigma} S(\psi)\Delta g\; d\sigma \quad \textbf{where}$$

$$S(\psi) = \frac{1}{\sin\frac{\psi}{2}} - 6\sin\frac{\psi}{2} + 1 - 5\cos\psi - 3\cos\psi\ln\left(\sin\frac{\psi}{2} + \sin^2\frac{\psi}{2}\right)$$

which was published by *George Gabriel Stokes in 1849* in his work "*On the variation of gravity on the surface of the Earth*", it is therefore called *Stokes' formula* and $S(\psi)$ then *Stokes' function*.

Nevertheless, soon the accuracy requirements where higher and the effort to solve the linearized problem for a better approximation of the boundary surface became a hot topic.

Many important results where obtained for the problem interpreted in a *spherical approximation* (considered as a mapping).

The problem was to find T such that

$$\Delta T = 0 \qquad \text{outside } \Gamma \quad \text{(telluroid in s. app.)}$$

$$|\boldsymbol{x}| \frac{\partial T}{\partial |\boldsymbol{x}|} + 2T = 2\Delta W - |\boldsymbol{x}|\,\Delta g \quad \text{on } \Gamma \quad \text{(telluroid in s. app.)}$$

and again the asymptotic condition at infinity was added, i.e.:

$$T = \frac{c}{|\boldsymbol{x}|} + O(|\boldsymbol{x}|^{-3}) \quad \text{for} \quad |\boldsymbol{x}| \to \infty$$

The solution methods and their use were given a considerable attention.

3. Integral Equation Method

In this approach, one represents T by a *single-layer potential*

$$T(\boldsymbol{x}) = \int_{\Gamma} \frac{1}{|\boldsymbol{x}-\boldsymbol{y}|} \mu(\boldsymbol{y})\, d_y\Gamma$$

and looks for the unknown density μ. This leads to the following integral equation:

$$2\pi\mu(\boldsymbol{x})\cos(\boldsymbol{x},\boldsymbol{n}_x) - \frac{3}{2|\boldsymbol{x}|}\int_{\Gamma} \frac{1}{|\boldsymbol{x}-\boldsymbol{y}|}\mu(\boldsymbol{y})\, d_y\Gamma -$$

$$- \frac{1}{2|\boldsymbol{x}|}\int_{\Gamma} \frac{|\boldsymbol{y}|^2 - |\boldsymbol{x}|^2}{|\boldsymbol{y}-\boldsymbol{x}|^3}\mu(\boldsymbol{y})\, d_y\Gamma = \Delta g$$

However, one soon realizes that an application of the *Riesz theorem of compact operator*, and the well-known *Fredholm alternatives* is associated with difficulties.

The second integral has a strongly singular kernel and thus *does not exist in the usual Lebesgue sense*.

4. Cauchy's Principal Value

The *Lebesgue integral* *does not depend* on how the partition of the integration domain is made finer. It represents a common value of the *infimum* of the upper and of the *supremum* of the lower Lebesgue sums.

***The idea cannot be applied* to integrals with strongly singular kernels.**

The strongly singular integral in our case can only be computed as *Cauchy's principal value*, usually symbolized by *v.p.* (*"valeur principale"*):

$$\text{v.p.} \int_{\Gamma} \frac{|\boldsymbol{y}|^2 - |\boldsymbol{x}|^2}{|\boldsymbol{y}-\boldsymbol{x}|^3} \mu(\boldsymbol{y})\, d_{\boldsymbol{y}}\Gamma = \lim_{\varepsilon \to 0} \int_{\Gamma - \Gamma_{\boldsymbol{x},\varepsilon}} \frac{|\boldsymbol{y}|^2 - |\boldsymbol{x}|^2}{|\boldsymbol{y}-\boldsymbol{x}|^3} \mu(\boldsymbol{y})\, d_{\boldsymbol{y}}\Gamma$$

where $\Gamma_{\boldsymbol{x},\varepsilon} \equiv \{\boldsymbol{y} \in \Gamma;\ |\boldsymbol{y}-\boldsymbol{x}| \le \varepsilon\}$

Some properties of an integral defined in the sense of *"valeur principale"* are illustrated in the following example.

5. Cauchy's Principal Value – Example

Assuming that $x \in (a,b)$, we obviously have

$$f(x) = \textbf{v.p.}\int_a^b \frac{d\xi}{\xi - x} = \lim_{\varepsilon \to 0}\int_a^{x-\varepsilon} \frac{d\xi}{\xi - x} + \lim_{\varepsilon \to 0}\int_{x+\varepsilon}^{b} \frac{d\xi}{\xi - x}$$

$$= \lim_{\varepsilon \to 0} \ln\frac{\varepsilon}{x-a} + \lim_{\varepsilon \to 0} \ln\frac{b-x}{\varepsilon} = \ln\frac{b-x}{x-a}$$

$$f'(x) = \frac{a-b}{(x-a)(b-x)} \quad \textbf{and} \quad f''(x) = \frac{(b-a)(a+b-2x)}{(a-x)^2(b-x)^2}$$

However,

$$\textbf{v.p.}\int_a^b \frac{d}{dx}\left(\frac{1}{\xi - x}\right) d\xi = -\ \textbf{p.v.}\int_a^b \frac{d\xi}{(\xi - x)^2} = -\infty$$

$$\textbf{v.p.}\int_a^b \frac{d^2}{dx^2}\left(\frac{1}{\xi - x}\right) d\xi = \textbf{p.v.}\int_a^b \frac{2\ d\xi}{(\xi - x)^3} = \frac{(b-a)(a+b-2x)}{(a-x)^2(b-x)^2}$$

6. Green's Function Method

Green's function can easily be constructed in cases that the *solution domain has an elementary shape*. It gives an explicit representation of the solution not only for *Laplaces'*, but also for *Poissons'* equation. *Indeed*, consider e.g. the following problem

$$\Delta T = g \quad \textbf{for} \quad |\boldsymbol{x}| > R \quad \textbf{and} \quad \frac{\partial T}{\partial |\boldsymbol{x}|} + \frac{2}{R} T = f \quad \textbf{for} \quad |\boldsymbol{x}| = R$$

Following principles in constructing Green's functions, we obtain

$$G(\boldsymbol{x}, \boldsymbol{y}) = \frac{1}{|\boldsymbol{x} - \boldsymbol{y}|} + \frac{R}{|\boldsymbol{x}|} \frac{1}{|\bar{\boldsymbol{x}} - \boldsymbol{y}|} - \frac{3R|\bar{\boldsymbol{x}} - \boldsymbol{y}|}{|\boldsymbol{x}||\boldsymbol{y}|^2} -$$

$$- \frac{R^3 \cos\psi}{|\boldsymbol{x}|^2 |\boldsymbol{y}|^2} \left[5 + 3 \ln \frac{1}{2} \left(1 - \frac{R^2 \cos\psi}{|\boldsymbol{x}||\boldsymbol{y}|} + \frac{|\bar{\boldsymbol{x}} - \boldsymbol{y}|}{|\boldsymbol{y}|} \right) \right]$$

where $\bar{\boldsymbol{x}} = \dfrac{R^2}{|\boldsymbol{x}|^2} \boldsymbol{x}$ **is given by an *inversion in a sphere*.**

The function $G(\boldsymbol{x},\boldsymbol{y})$ enables us to *express the solution of our problem explicitly*. The natural point of departure is a (slightly modified) *Green's third identity*

$$T(\boldsymbol{x}) = -\frac{1}{4\pi}\int_{|\boldsymbol{y}|>R} G(\boldsymbol{x},\boldsymbol{y})\Delta T(y)\,d\boldsymbol{y} -$$

$$-\frac{1}{4\pi}\int_{|\boldsymbol{y}|=R}\left[G(\boldsymbol{x},\boldsymbol{y})\frac{\partial T(\boldsymbol{y})}{\partial|\boldsymbol{y}|} - T(\boldsymbol{y})\frac{\partial G(\boldsymbol{x},\boldsymbol{y})}{\partial|\boldsymbol{y}|}\right]d_yS$$

For $G(\boldsymbol{x},\boldsymbol{y})$ as above the formula immediately yields

$$T(\boldsymbol{x}) = T_1(\boldsymbol{x}) - \frac{1}{4\pi}\int_{|\boldsymbol{y}|=R} G(\boldsymbol{x},\boldsymbol{y})\,f(\boldsymbol{y})\,d_yS - \frac{1}{4\pi}\int_{|\boldsymbol{y}|>R} G(\boldsymbol{x},\boldsymbol{y})g(\boldsymbol{y})\,d\boldsymbol{y}$$

***Note.* The restriction of $G(\boldsymbol{x},\boldsymbol{y})$ for $|\boldsymbol{y}| = R$ or $|\boldsymbol{x}| = |\boldsymbol{y}| = R$ attains the form of *the (Pizzetti extended) Stokes function* or *the classical Stokes function*, respectively.**

7. Green's Function and a More General Boundary

Green's function $G(\boldsymbol{x},\boldsymbol{y})$ is essentially associated with our problem considered for a sphere of radius R . *Nevertheless,* $G(\boldsymbol{x},\boldsymbol{y})$ *can be also useful in a more general case*. This can be shown by means of a transformation of coordinates

$$y_i = y_i(x_1, x_2, x_3) \quad , \quad i = 1, 2, 3$$

***that gives the geodetic boundary-value problem* the structure of our simple problem, i.e.**

$$\Delta_{\boldsymbol{y}} T = g \quad \textbf{for} \quad |\boldsymbol{y}| > R \quad \textbf{and} \quad \frac{\partial T}{\partial |\boldsymbol{y}|} + \frac{2}{R} T = f^* \quad \textbf{for} \quad |\boldsymbol{y}| = R$$

with the only difference that

$$g = g(T) = \delta^{ij} \frac{\partial^2 T}{\partial y_i \partial y_j} - g^{ij} \left(\frac{\partial^2 T}{\partial y_i \partial y_j} - \Gamma_{ij}^k \frac{\partial T}{\partial y_k} \right)$$

where the *metric tensor* g^{ij} and the *Christoffel symbols* Γ_{ij}^k depend on the geometry of the original boundary (the telluroid).

Clearly, the representation formula now changes into an *integro-differential* equation.

$$T(\boldsymbol{y}) = T_1(\boldsymbol{y}) - \frac{1}{4\pi} \int_{|\xi| = R} G(\boldsymbol{y}, \boldsymbol{\xi})\, f^*(\boldsymbol{\xi})\, d_{\xi} S \; -$$

$$- \frac{1}{4\pi} \int_{|\xi| > R} G(\boldsymbol{y}, \boldsymbol{\xi})\, g\left[T(\boldsymbol{\xi}), \frac{\partial T(\boldsymbol{\xi})}{\partial \xi_i}, \frac{\partial^2 T(\boldsymbol{\xi})}{\partial \xi_i \partial \xi_j} \right] d\boldsymbol{\xi}$$

In both the cases, i.e.

integral equation method **and** ***Green's function method*****,**

the solution leads to an *iteration process*. Nevertheless, for the method that rests on Greens' function all the integrals involved exist in the usual Lebesgue sense.

8. Weak Solution

In gravity field studies the approach to boundary-value problems for Laplace's (or Poisson's) equation often represents what is known as a *classical solution*. - We look for a smooth function satisfying the differential equation and the boundary condition *"pointwise"*. The method of integral equations and Green's function method are most frequently used.

Alternatively, we can look for *a measurable function satisfying a certain integral identity* connected with the boundary-value problem in question. This is the so-called *weak solution*. Natural function spaces corresponding to this method are *Sobolev's spaces*.

In many cases there even exists a possibility to replace the integration of a differential equation under given boundary conditions by an *equivalent problem* of getting *a function that minimizes some integral*. This corresponds to *variational methods*.

Historically, the first use of *variational methods* was in the form of *Dirichlet's principle*. *According to this principle:* among functions which attain given values on the boundary $\partial\Omega$ of a domain Ω, that and only that function which is harmonic in Ω minimizes the so-called *Dirichlet's integral:*

$$\int_{\Omega} \sum_{i=1}^{3} \left(\frac{\partial u}{\partial x_i} \right)^2 d\boldsymbol{x}$$

Dirichlet's principle was extensively used by

***Riemann (1826-1866),* but critically commented by**

Weierstrass (1815-1897)* and later by *Hadamard (1865-1963).

In the beginning of the 20th century the principle got a new interest. *Hilbert (1862-1943)* showed that the *justification* of Dirichlet's principle *is essentially associated* with the notion of the *completeness of the metric space.*

The justification by Hilbert has a close tie to his contributions to the development of the calculus of variations, see Giaquinta (2000): Hilbert e il calcolo delle variazioni. Le Matematiche, Vol. LV, Supplemento n. 1, pp. 47-58.

Nevertheless, our intention is to discuss problems associated with the determination of the external gravity field of the Earth. In consequence we have to suppose that Ω mentioned above is an *unbounded solution domain*.

As regards functions spaces, we will work with functions from *Sobolev's weighted* space $W_2^{(1)}(\Omega)$ endowed with inner product

$$(u,v)_1 \equiv \int_{\Omega} \frac{uv}{|\boldsymbol{x}|^2}\, d\boldsymbol{x} + \sum_{i=1}^{3} \int_{\Omega} \frac{\partial u}{\partial x_i} \frac{\partial v}{\partial x_i}\, d\boldsymbol{x}$$

Also the boundary $\partial\Omega$ of the domain Ω will be supposed to have a certain degree of regularity. Putting $\Omega' = \boldsymbol{R}^3 - \Omega \cup \partial\Omega$, we will suppose that Ω' is a domain with *Lipschitz' boundary.*

9. Example - Neumann's Problem and a Quadratic Functional

Put

$$A(u,v)=\sum_{i=1}^{3}\int_{\Omega}\frac{\partial u}{\partial x_i}\frac{\partial v}{\partial x_i}\,d\boldsymbol{x}$$

which is a *bilinear form* on $W_2^{(1)}(\Omega)\times W_2^{(1)}(\Omega)$ **and consider the quadratic functional**

$$\Phi(u)=A(u,u)-2\int_{\partial\Omega}uf\,dS$$

defined on $W_2^{(1)}(\Omega)$**, where** $f\in L_2(\partial\Omega)$**.**

The functional Φ ***attains its minimum in*** $W_2^{(1)}(\Omega)$ **(which results from the theory of an abstract variational problem).**

Conversely, assuming that Φ **has its local minimum at a point** $u\in W_2^{(1)}(\Omega)$**, we necessarily arrive at**

$$A(u,v) = \sum_{i=1}^{3} \int_{\Omega} \frac{\partial u}{\partial x_i} \frac{\partial v}{\partial x_i} \, d\boldsymbol{x} = \int_{\partial\Omega} vf \; dS$$

valid for all $v \in W_2^{(1)}(\Omega)$**.**

This integral identity represents *Euler's necessary condition* for Φ **to have a minimum at the point** u**. It has also a classical interpretation. Under some regularity assumptions one can apply Green's identity and show then that** u **has to be a solution of *Neumann's (exterior) problem*, i.e.,**

$$\Delta u = 0 \quad \text{in} \quad \Omega$$

and

$$\frac{\partial u}{\partial n} = -f \quad \text{on} \quad \partial\Omega$$

where Δ **means Laplace's operator and** $\partial / \partial n$ **denotes the derivative in the direction of the unit normal** $\boldsymbol{n}$ **of** $\partial\Omega$**.**

10. An Oblique Derivative Problem

In studies on Earth gravity field, however, we are faced by a rather complex reality. We will consider the *linear gravimetric boundary-value problem* (which is a *fix boundary value problem*) and try to show its tie to the explanations above.

Let W and U be the gravity and the standard potential of the Earth, respectively. Thus

$g = \lvert \boldsymbol{grad}\, W \rvert$	**is the measured gravity,**
$\gamma = \lvert \boldsymbol{grad}\, U \rvert$	**means the normal gravity,**
$T(\boldsymbol{x}) = W(\boldsymbol{x}) - U(\boldsymbol{x})$	**is the disturbing potential,**
$\delta g(\boldsymbol{x}) = g(\boldsymbol{x}) - \gamma(\boldsymbol{x})$	**is the gravity disturbance.**

We assume that g is corrected for the gravitational interaction with the Moon, the Sun and the planets, for the precession and nutation of the Earth and so on.

The solution domain Ω is the exterior of the Earth and our problem is to find T such that

$$\Delta T = 0 \quad \text{in} \quad \Omega$$

$$\left\langle \boldsymbol{s}, \boldsymbol{grad}\, T \right\rangle = -\,\delta g \quad \text{on} \quad \partial\Omega$$

where $\boldsymbol{s} = -\left(1/\gamma\right) \boldsymbol{grad}\, U$, $\left\langle .,. \right\rangle$ is the inner product in $\boldsymbol{R}^3$ and T is assumed regular as $\boldsymbol{x} \to \infty$, in particular $T = \mathcal{O}(|\,\boldsymbol{x}\,|^{-1})$.

Following the weak formulation, **we will assume that on $W_2^{(1)}(\Omega) \times W_2^{(1)}(\Omega)$ we have a bilinear form $A(u,v)$ such that our problem may be written in terms of an integral identity**

$$A(T,v) = \int_{\partial\Omega} vf \; dS \qquad (.)$$

valid for all $v \in W_2^{(1)}(\Omega)$. Its solution is sought as a function $T \in W_2^{(1)}(\Omega)$ and f is assumed square integrable on $\partial\Omega$.

However, ***the gravimetric boundary-value problem is an oblique derivative problem*** **and for this reason we have to put**

$$A(u,v) = A_1(u,v) - A_2(u,v)$$

where

$$A_1(u,v) = \int_\Omega \langle \boldsymbol{grad}\, u, \boldsymbol{grad}\, v \rangle \, d\boldsymbol{x}$$

$$A_2(u,v) = \int_\Omega \langle \boldsymbol{grad}\, v, \boldsymbol{a} \times \boldsymbol{grad}\, u \rangle \, d\boldsymbol{x} + \int_\Omega v \langle \boldsymbol{curl}\, \boldsymbol{a}, \boldsymbol{grad}\, u \rangle \, d\boldsymbol{x}$$

and $\boldsymbol{a} = (a_1, a_2, a_3)$ **is a vector field such that** a_i **and also** $|\boldsymbol{x}|(\boldsymbol{curl}\ \ \boldsymbol{a})_i$, $i = 1,\ 2,\ 3$, **are Lebesgue measurable functions defined and bounded almost everywhere on** Ω**.**

Moreover, we assume that on the boundary $\partial\Omega$ **the vector** $\boldsymbol{\sigma} = \boldsymbol{s} / \langle \boldsymbol{s}, \boldsymbol{n} \rangle$ **and the field** $\boldsymbol{a}$ **are coupled so that** $\boldsymbol{\sigma} = \boldsymbol{n} + \boldsymbol{a} \times \boldsymbol{n}$**.**

Note also that the tie to the classical formulation above requires that $f = \gamma(\partial U / \partial n)^{-1} \delta g$**.**

Let us consider now a sequence **of functions** $[u_m]_{m=0}^{\infty}$ **defined by the following equations**

$$A_1(u_{m+1}, v) = \int_{\partial\Omega} vf \; dS + A_2(u_m, v)$$

which are assumed to hold for all $v \in W_2^{(1)}(\Omega)$ **and** $m = 0,\ 1, \ldots, \infty$**.**

Under some limitations one can even show that

$$\| u_{m+2} - u_{m+1} \|_1 \leq c \| u_{m+1} - u_m \|_1$$

where c **is a positive constant such that** $c < 1$ **. Then**

$$\| u_{m+2} - u_{m+1} \|_1 \leq c^{m+1} \| u_1 - u_0 \|_1$$

so that for any integer $p > 0$

$$\| u_{m+p} - u_{m+1} \|_1 \leq \frac{c^{m+1}}{1-c} \| u_1 - u_0 \|_1$$

and it follows immediately that $\| u_{m+p} - u_{m+1} \|_1 \to 0$ **as** $m \to \infty$**.**

This means that:

$[\, u_m \,]_{m=0}^{\infty}$ **is a *Cauchy sequence* in** $W_2^{(1)}(\Omega)$ **and in the norm** $\|\,.\,\|_1 = (\,.\,,\,.\,)_1^{1/2}$ **it converges to a function** $u \in W_2^{(1)}(\Omega)$**, which is the solution of our weakly formulated problem.**

Under certain regularity assumptions **the iterations may be even interpreted as follows:**

$$A_1(u_{m+1}, v) = \int_{\partial\Omega} v f_m \, dS \quad \text{is valid for all} \quad v \in W_2^{(1)}(\Omega)$$

while

$$f_m = f - \frac{\partial u_m}{\partial t} \tan(\boldsymbol{s}, \boldsymbol{n})$$

with $\partial / \partial t$ **denoting the derivative in the direction of** $\boldsymbol{t} = (\boldsymbol{\sigma} - \boldsymbol{n}) / |\boldsymbol{\sigma} - \boldsymbol{n}|$ **- which obviously is tangential to** $\partial\Omega$ **(and exists almost everywhere on Lipschitz' boundary** $\partial\Omega$**).**

11. Linear System

In the sequel it is enough to consider just a space $H_2^{(1)}(\Omega)$ of those functions from $W_2^{(1)}(\Omega)$ which are harmonic in Ω and to reformulate our problem, i.e. to look for $u_{m+1} \in H_2^{(1)}(\Omega)$ such that

$$A_1(u_{m+1}, v) = \int_{\partial\Omega} v f_m \, dS$$

holds for all $v \in H_2^{(1)}(\Omega)$. We will approximate u_{m+1} by means of

$$u^{(n,m)} = \sum_{j=1}^{n} c_j^{(n,m)} v_j$$

where v_j are members of a function basis of $H_2^{(1)}(\Omega)$ and the coefficients $c_j^{(n,m)}$ can be obtained from *Galerkin's system*

$$\sum_{j=1}^{n} c_j^{(n,m)} A_1(v_j, v_k) = \int_{\partial\Omega} v_k f_m \, dS \,, \quad k = 1, \ldots, n$$

In practice a modification of the bilinear form $A_1(u,v)$ ***is useful,*** **to simplify the computation of** $A_1(v_j, v_k)$**. In particular put**

$$A^*(u,v) = \int_{\Omega^*} \langle \boldsymbol{grad}\, u, \boldsymbol{grad}\, v \rangle \, d\boldsymbol{x} \quad \text{for} \quad u,v \in H_2^{(1)}(\Omega^*)$$

where Ω^* **has a "*simpler boundary*". However, for** v_j **we have to take members of a function basis in** $H_2^{(1)}(\Omega^*)$**. In** $H_2^{(1)}(\Omega^*)$ **they generate a sequence of finite dimensional subspaces**

$$H_n(\Omega^*) = \operatorname{span}\{v_i, i = 1, \ldots, n\}, \quad n = 1, 2, \ldots$$

We will suppose that $\Omega \subseteq \Omega^*$**. Thus, using *Runge's property* of Laplace's equation, we can take** v_j **(restricted to** Ω**) as members of a function basis in** $H_2^{(1)}(\Omega)$ **too. By analogy then**

$$H_n(\Omega) = \operatorname{span}\{v_i, i = 1, \ldots, n\}, \quad n = 1, 2, \ldots$$

and it is clear that $H_n(\Omega) = H_n(\Omega^*)\Big|_{\Omega}$**.**

Thus for all $v \in H_n(\Omega^*)$

$$A^*(u^{(n,m)}, v) = \int_{\partial\Omega} v f_m \, dS + F(v) \qquad \textbf{(..)}$$

where

$$F(v) = A^*(u^{(n,m)}, v) - A_1(u^{(n,m)}, v) = \int_D \langle \boldsymbol{grad}\, u^{(n,m)}, \boldsymbol{grad}\, v \rangle \, d\boldsymbol{x}$$

and $D = \Omega^* - \Omega$**. The Eqs. above imply a continuation of** $u^{(n,m)}$**, and *Eq. (..) is an alternative expression of the original system.***

12. Successive Approximations

Our aim is to solve the integral identity (..) by successive approximations. *Therefore,* we will examine the sequence of functions

$$u_0^{(n,m)},\ u_1^{(n,m)},\ \cdots,\ u_k^{(n,m)},\ u_{k+1}^{(n,m)},\ \cdots$$

defined by

$$A^*(u_{k+1}^{(n,m)}, v) = \int_{\partial\Omega} v f_m \, dS + F_k(v) \quad \textbf{valid for all} \quad v \in H_n(\Omega^*)$$

where

$$F_k(v) = \int_D \langle \boldsymbol{grad}\, u_k^{(n,m)}, \boldsymbol{grad}\, v \rangle \, d\boldsymbol{x}$$

Does the sequence $[u_k^{(n,m)}]_{k=0}^{\infty}$ ***have a limit?*** **We first deduce that**

$$A^*(u_{k+2}^{(n,m)} - u_{k+1}^{(n,m)}, v) = \overline{F}(v)$$

where

$$\overline{F}(v) = \int_D \langle \boldsymbol{grad}\,(u_{k+1}^{(n,m)} - u_k^{(n,m)}), \boldsymbol{grad}\, v \rangle \, d\boldsymbol{x}$$

holds for all $v \in H_n(\Omega^*)$**. It is clear that for** $u_{k+1}^{(n,m)} - u_k^{(n,m)}$ **fixed,** $\overline{F}(v)$ **is a bounded linear functional of the variable** v**. Indeed, using *Hölder's inequality*, we easily obtain that**

$$|\bar{F}(v)| \le M \sqrt{\int_D |\boldsymbol{grad}\, v|^2 \, d\boldsymbol{x}} \le M \, \| v \|_{H_2^{(1)}(\Omega^*)}$$

where

$$M = \sqrt{\int_D |\boldsymbol{grad}\,(u_{k+1}^{(n,m)} - u_k^{(n,m)})|^2 \, d\boldsymbol{x}}$$

Thus the norm $\| \bar{F} \|$ of $\bar{F}$ can be estimated from above by M, i.e. $\| \bar{F} \| \le M$. More than that, for functions of *band limited spectrum* we even have

$$|\bar{F}(v)| \le M \sqrt{\mu} \, \| v \|_{H_2^{(1)}(\Omega^*)}$$

where,

$$M \le \sqrt{\mu} \, \| u_{k+1}^{(n,m)} - u_k^{(n,m)} \|_{H_2^{(1)}(\Omega^*)}$$

and this immediately yields

$$\| \bar{F} \| \le \mu \, \| u_{k+1}^{(n,m)} - u_k^{(n,m)} \|_{H_2^{(1)}(\Omega^*)}$$

Return now to the bilinear form $A^*(u,v)$ **and assume that** $\Omega' = \boldsymbol{R}^3 - \bar{\Omega}^*$ **is a star-shaped domain with respect to the origin with Lipschitz' boundary.** ***Under this assumption***

$$\| v \|^2_{W_2^{(1)}(\Omega^*)} \le \alpha \int_{\Omega^*} | \boldsymbol{grad}\, v |^2 \, d\boldsymbol{x}$$

for all $v \in W_2^{(1)}(\Omega^*)$ **with** $\alpha = 5$ **. Hence**

$$A^*(u,u) \ge \frac{1}{\alpha} \| u \|^2_{H_2^{(1)}(\Omega^*)}$$ **holds for all** $u \in H_2^{(1)}(\Omega^*)$

which means that $A^*(u,v)$ ***is an elliptic bilinear form.***

Moreover, one can also verify that

$$A^*(u,v) \le \| u \|_{H_2^{(1)}(\Omega^*)} \| v \|_{H_2^{(1)}(\Omega^*)}$$

The properties of $A^*(u,v)$ and the boundedness of $\overline{F}(v)$ make it possible to apply *Lax-Milgram's theorem*. It allows us to deduce

$$\| u_{k+2}^{(n,m)} - u_{k+1}^{(n,m)} \|_{H_2^{(1)}(\Omega^*)} \le \alpha \| \overline{F} \| \le c \| u_{k+1}^{(n,m)} - u_k^{(n,m)} \|_{H_2^{(1)}(\Omega^*)}$$

where $c = \alpha\mu$. In consequence for any integer $p > 0$

$$\| u_{k+p}^{(n,m)} - u_{k+1}^{(n,m)} \|_{H_2^{(1)}(\Omega^*)} \le \frac{c^{k+1}}{1-c} \| u_1^{(n,m)} - u_0^{(n,m)} \|_{H_2^{(1)}(\Omega^*)}$$

which yields $\| u_{k+p}^{(n,m)} - u_{k+1}^{(n,m)} \|_{H_2^{(1)}(\Omega^*)} \to 0$ for $k \to \infty$, provided that $c < 1$. Thus $[u_k^{(n,m)}]_{k=0}^{\infty}$ *is a Cauchy sequence in* $H_2^{(1)}(\Omega^*)$ and clearly, it converges to a function $u \in H_2^{(1)}(\Omega^*)$. Note that $\Omega \subseteq \Omega^*$.

Obviously, the problem which needs discussion is the magnitude of the parameters α and μ in combination with the condition $c = \alpha\mu < 1$.

13. Numerical simulations – Case I

(*i*) In quality of the domain Ω the exterior of the *ETOPO5* surface is used.

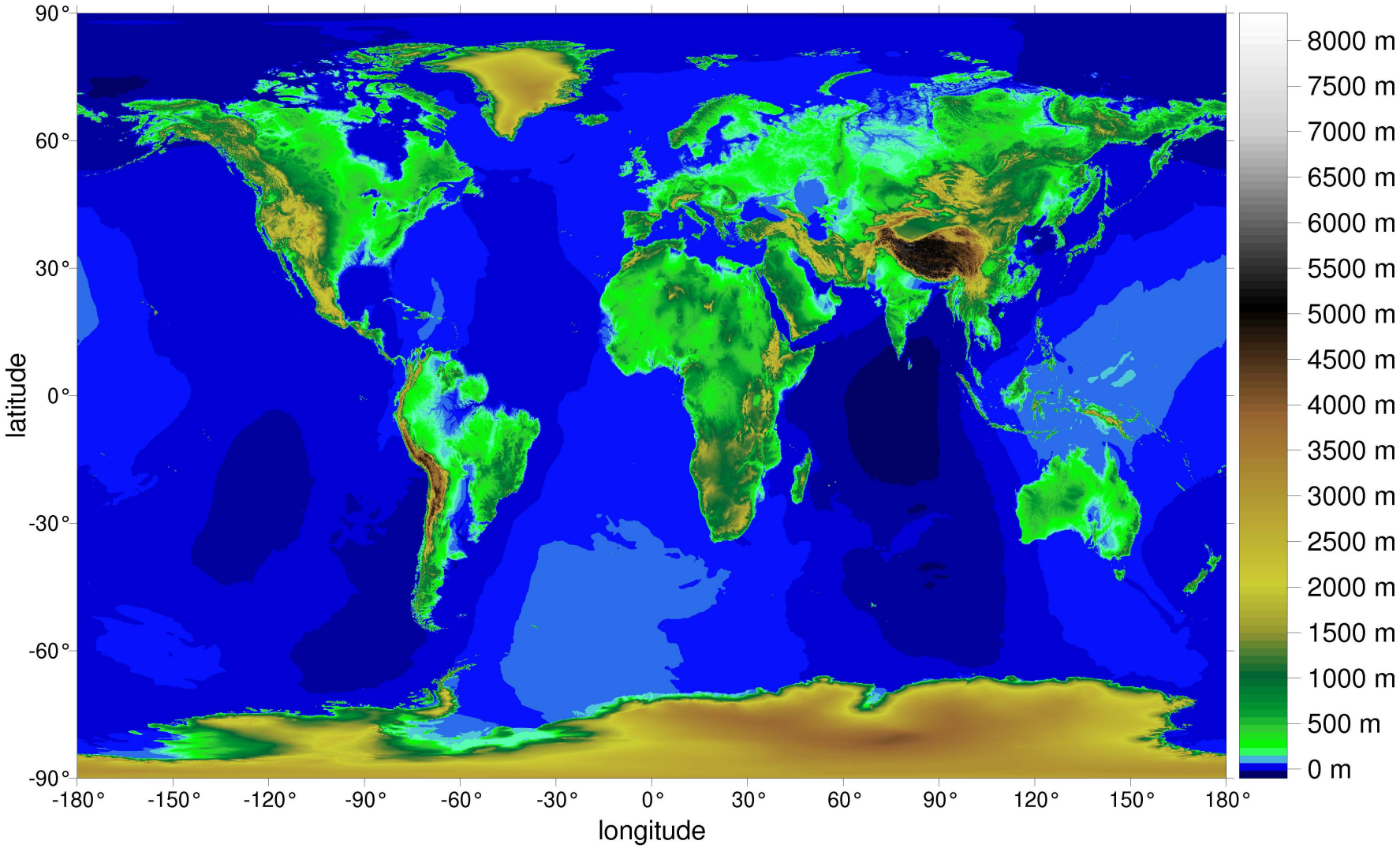

(*ii*) The real gravity potential W is simulated by *EGM96* and the input data on the *ETOPO5* - boundary surface are given by $\delta g = |\,\boldsymbol{grad}\,W\,| - |\,\boldsymbol{grad}\,U\,|$ (with U referred to *GRS80*).

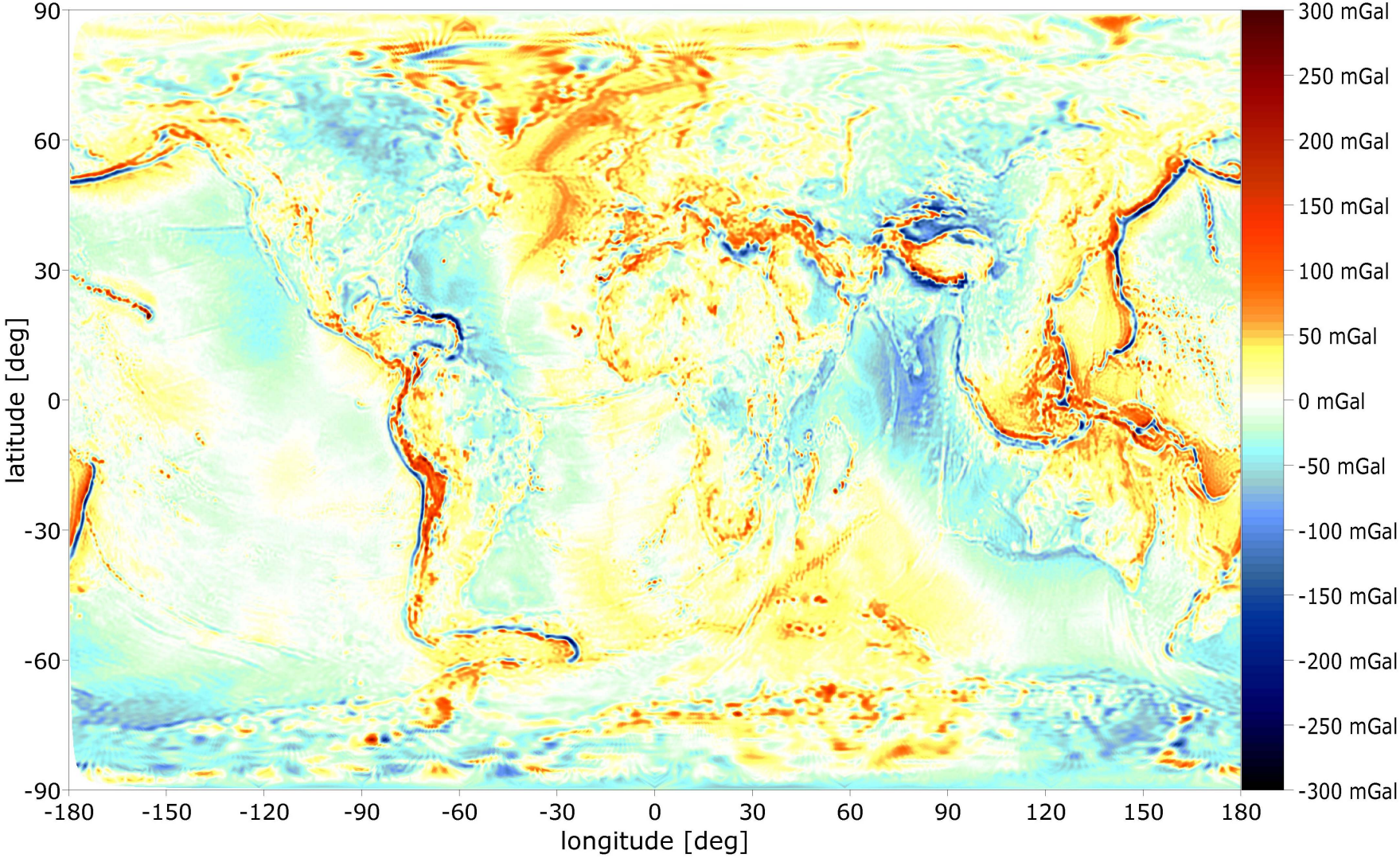

(*iii*) Surface integrals on the R.H.S. of Galerkin's system of linear equations.

For the numerical integration vertices of an *icosahedron* are projected onto the boundary surface. The triangles obtained in this way are used for generating *hierarchical triangulation* of the boundary.

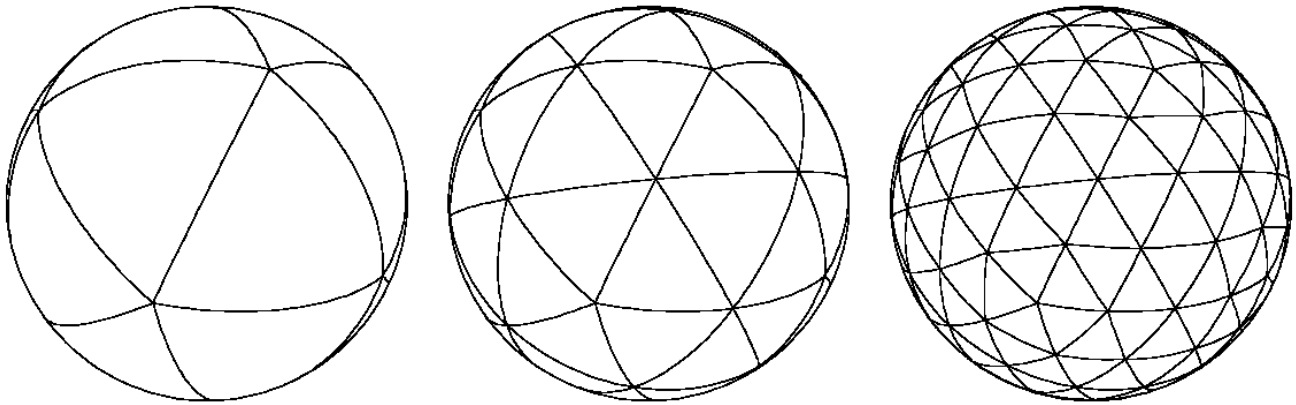

The surface integration then exploits principles of *Romberg's method* combined with *Richardson's extrapolation* up to the limit. It increases the accuracy and provides feedback in the control of the integration error.

(*iv*) For the domain Ω^* that has a "*simpler boundary* " $\partial\Omega^*$ we take the *sphere of radius* R .

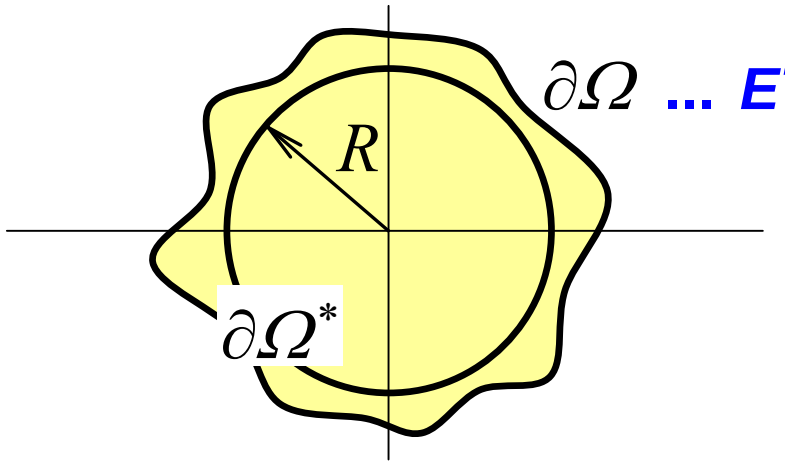

***Recall* that in this case one can easily compute the *reproducing kernel* of the function space $H_2^{(1)}(\Omega^*)$. Indeed, for $|\boldsymbol{x}| \geq R$**

$$K(\boldsymbol{x},\boldsymbol{y}) = \frac{1}{4\pi R}\sum_{n=0}^{\infty}\frac{2n+1}{n+1} z^{n+1} P_n(\cos\psi)$$ **, where** $|\boldsymbol{y}| > R$ **,**

$z = \dfrac{R^2}{|\boldsymbol{x}||\boldsymbol{y}|}$ **and** ψ **is the angle between** $\boldsymbol{y}$ **and** $\boldsymbol{x}$ **.**

In addition we also know that

$$K(\boldsymbol{x},\boldsymbol{y}) = \frac{1}{4\pi R}\left(\frac{2z}{L} - \ln\frac{L+z-\cos\psi}{1-\cos\psi}\right) ,$$

where $L = (1-2z\cos\psi + z^2)^{1/2}$ **.**

Recall in particular* that the reproducing kernel** $K(\boldsymbol{x},\boldsymbol{y})$ ***generates a function basis

$$v_i(\boldsymbol{x}) = K(\boldsymbol{x},\boldsymbol{y}_i) \ , \quad i = 1,2,\ldots,n \ ,$$

in the space $H_2^{(1)}(\Omega^*)$ **,** ***which is very suitable for approximation purposes.*** **Moreover, basis functions of this kind yield entries in *Galarkin's matrix* in a very straightforeword way.**

Note finally* that in our simulations the *parking grid* of the points** $\boldsymbol{y}_i$ **,** $i = 1,2,\ldots,n$ **, is given by vertices of the *6th level of the icosahedron refinement*, so that the *dimension of the subspace $H_n(\Omega^*) = \mathrm{span}\{v_i,\ i = 1,\ldots,n\}$ **is** $\boldsymbol{n} = \mathbf{40962}$ **.** ← **!!!**

(*v*) Structure of *Galerkin's matrix* for the approximation space $H_n(\Omega^*)$ of dimension $n = 40962$ generated by the *reproducing kernel* $K(x, y)$

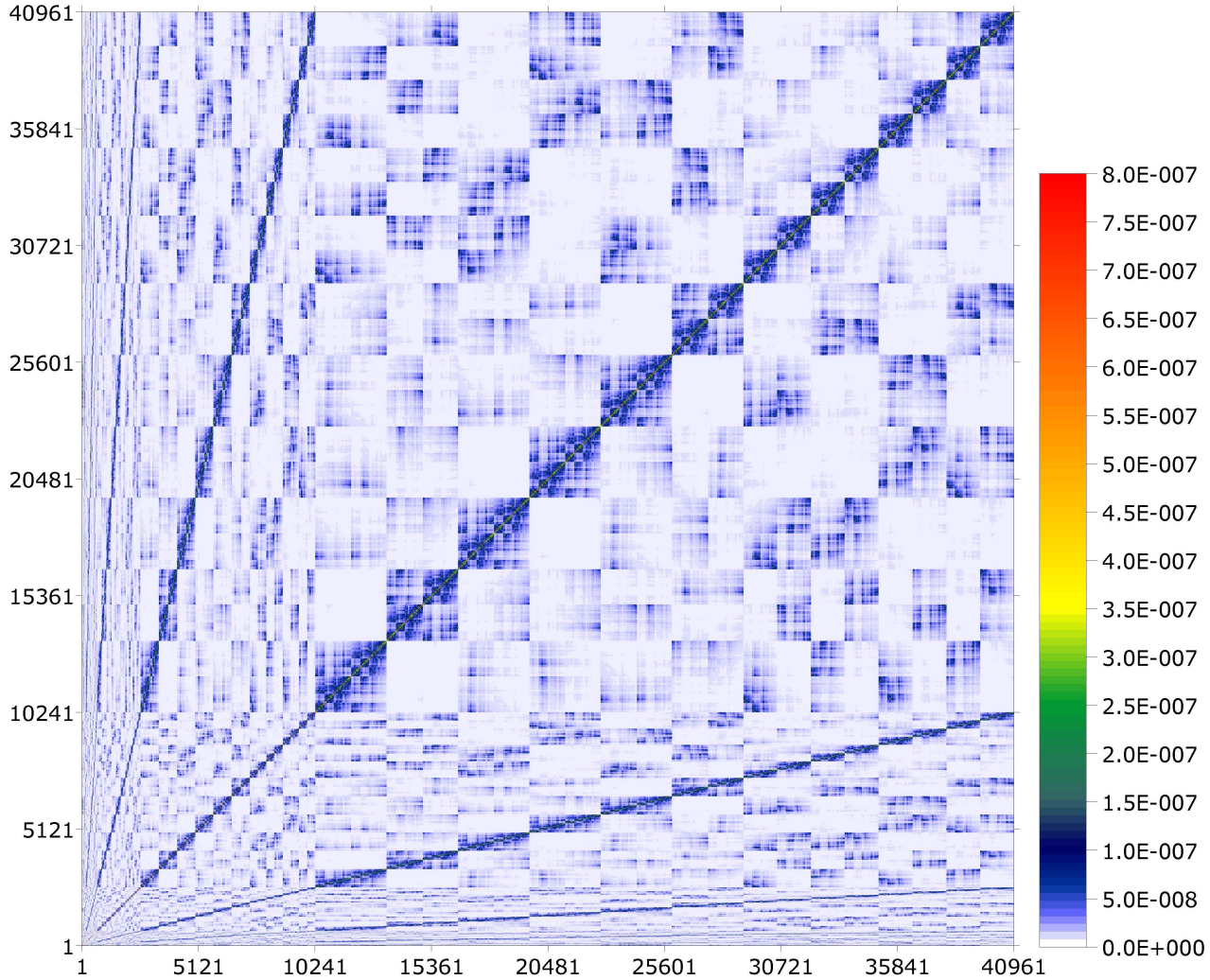

14. Case I - Experiments

In our numerical simulations the disturbing potential $T = W - U$ is known. The figure shows its values on the *ETOPO5* - surface.

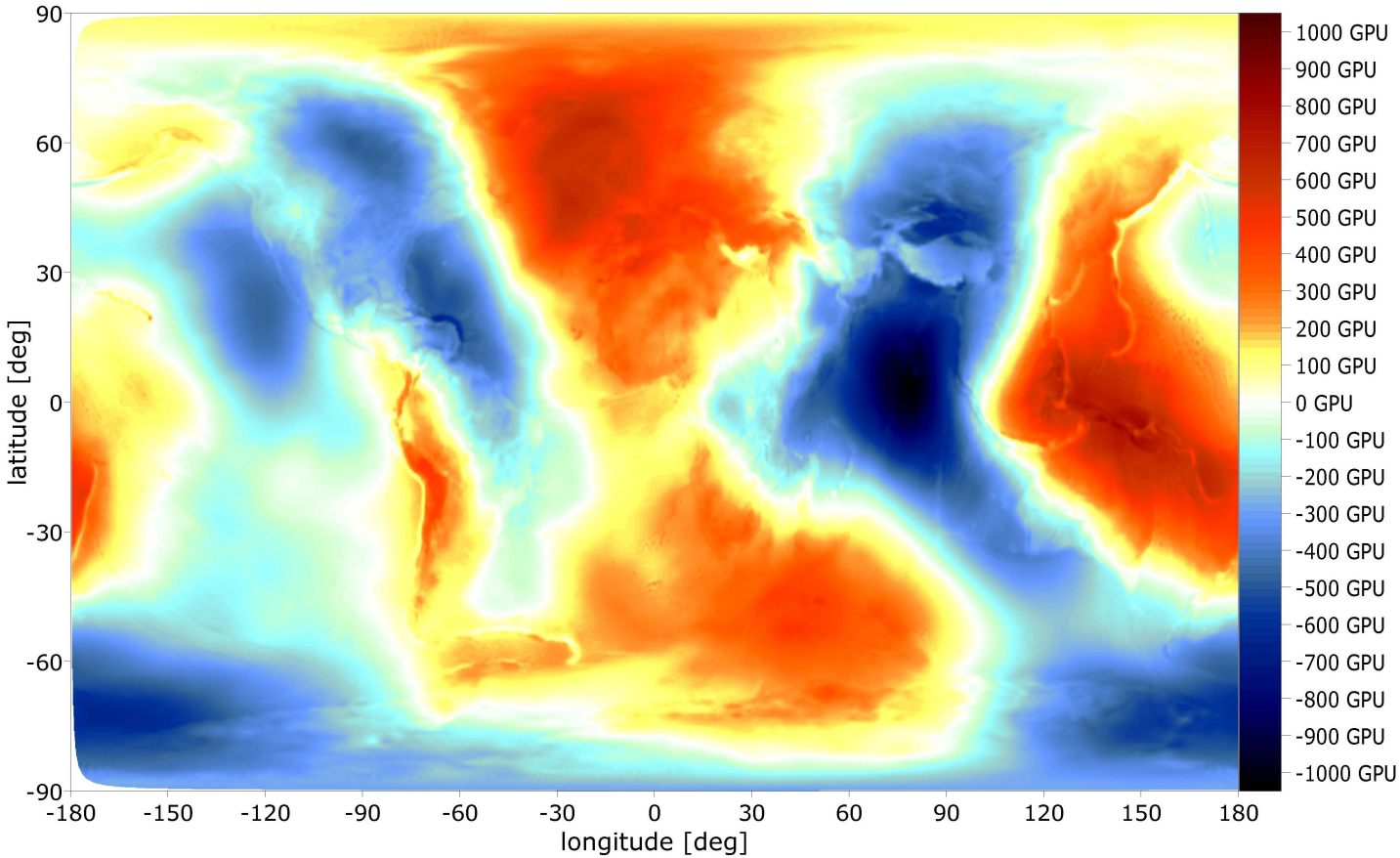

T is used as an "*exact* " solution and in the sequel is confronted with the outcome of individual *iteration steps*.

1st Iteration Step: **Comparison of the exact T with T_1**

The initial approximation $T_0 = 0$, so that we obtain T_1 from

$$A^*(T_1^{(n)}, v) = \int_{\partial\Omega} v \frac{1}{\langle \boldsymbol{s}, \boldsymbol{n} \rangle} \delta g \, dS$$ **valid for all $v \in H_n(\Omega^*)$.**

The dimension of the approximation space $H_n(\Omega^*)$ is

$\boldsymbol{n} = \mathbf{40962}$ **.**

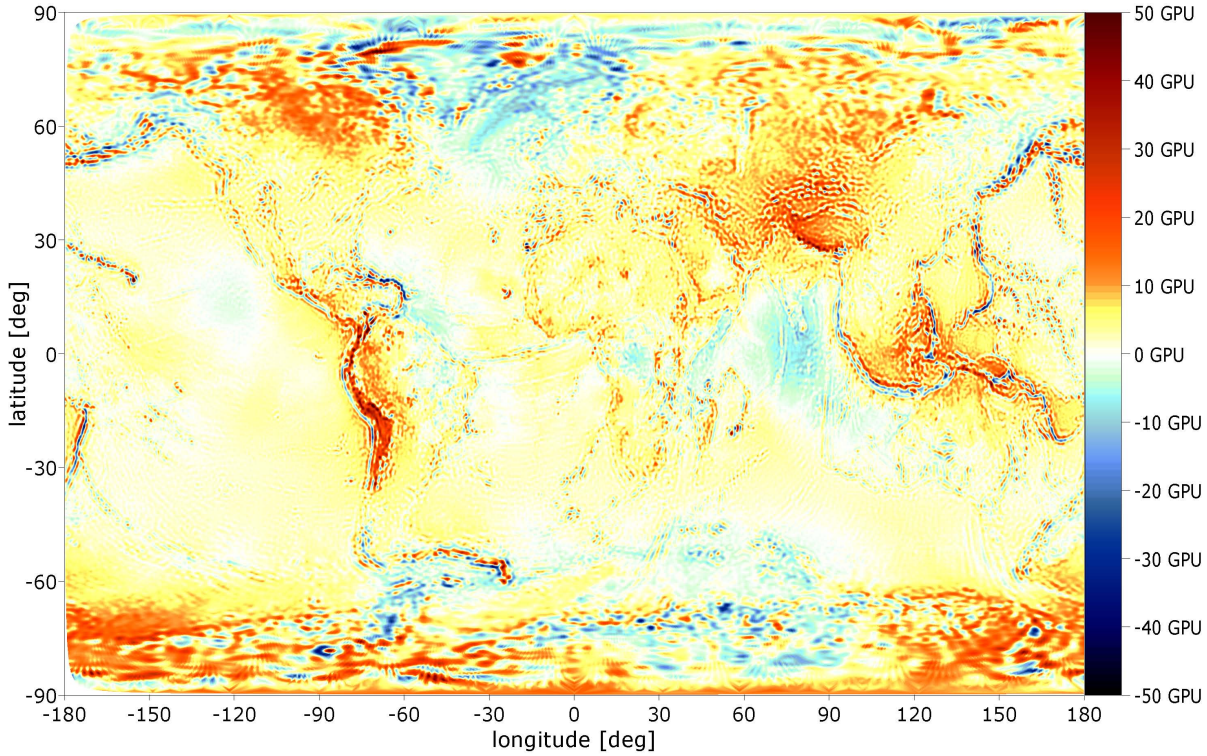

Characteristics: **min** $-51\,GPU$ **, max** $89\,GPU$ **, rms** $6.1\,GPU$

2nd Iteration Step: **Comparison of the exact T with T_3**

Here T_3 is defined for all $v \in H_n(\Omega^*)$ by

$$A^*(T_3^{(n)} - T_2^{(n)}, v) = \int_{\partial\Omega} v \frac{1}{\langle \boldsymbol{s}, \boldsymbol{n} \rangle} [\delta g + \langle \boldsymbol{s}, \boldsymbol{grad}\, T_2^{(n)} \rangle] \, dS \quad ,$$

The dimension of the approximation space $H_n(\Omega^*)$ is

$\boldsymbol{n} = \mathbf{40962}$ **.**

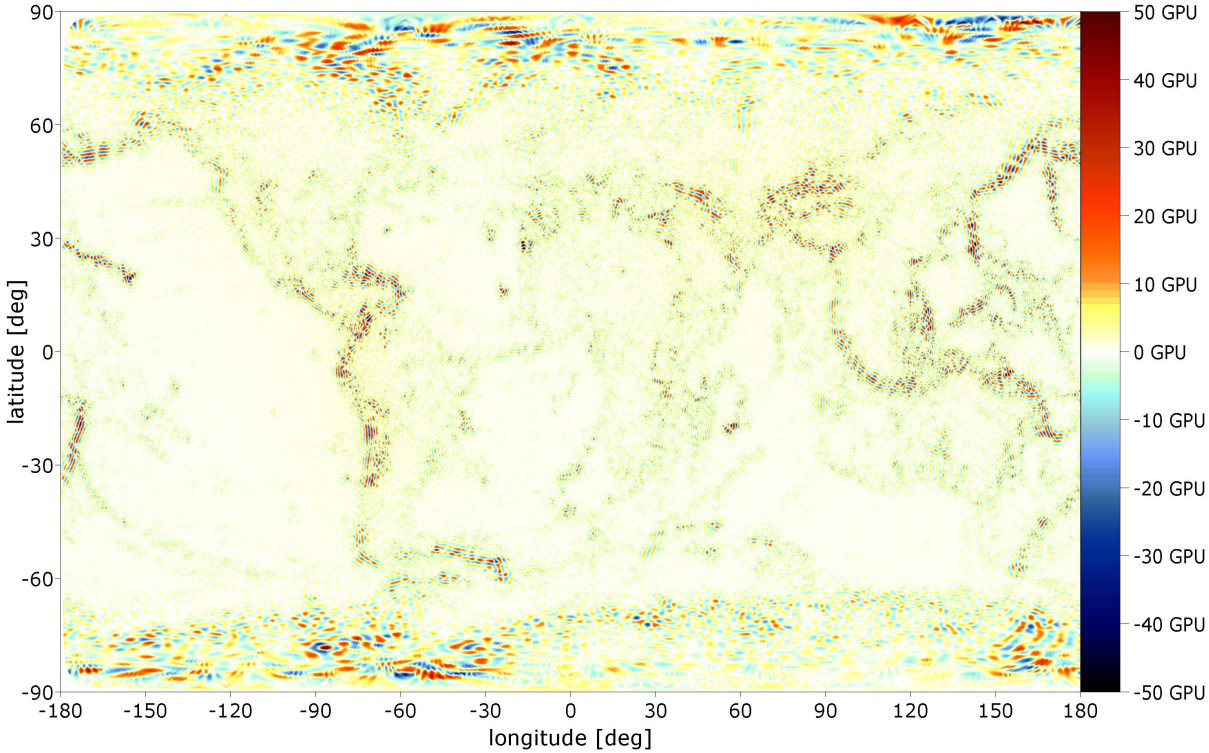

Characteristics: **min** $-49\ GPU$ **,** **max** $62\ GPU$ **,** **rms** $3.7\ GPU$

15. Numerical Simulation – Case II

(*i*) For the domain Ω^* that has a "*simpler boundary*" $\partial\Omega^*$ an *ellipsoid of revolution* has been taken.

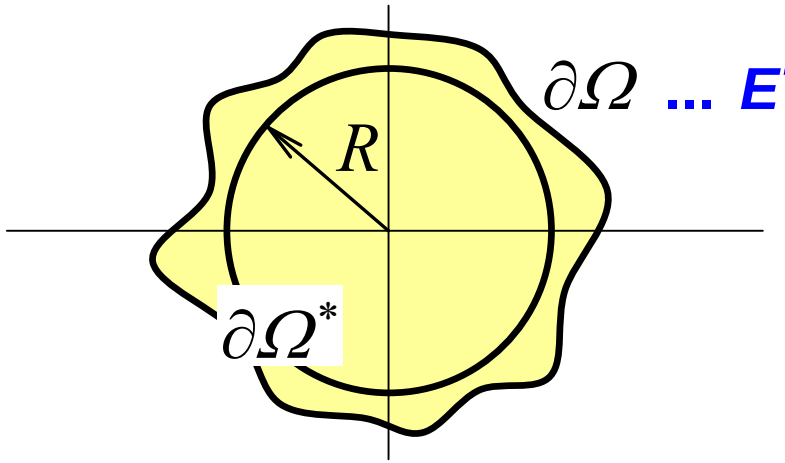

(*ii*) The potential $T = W - U$ as the "*exact*" solution has been derived from *EGM08*.

(*iii*) *The function basis* of the approximation space $H_n(\Omega^*)$ has been generated by the reciprocal distance, i.e.

$$v_i(\boldsymbol{x}) = \frac{1}{|\boldsymbol{x} - \boldsymbol{y}_i|} \quad , \quad i = 1, 2, \ldots, n \quad \text{with} \quad \boldsymbol{n} = \mathbf{163842}$$

(*iv*) *Parking grid* for basis functions in the approximation space $H_n(\Omega^*)$ of dimension $n = 163842$

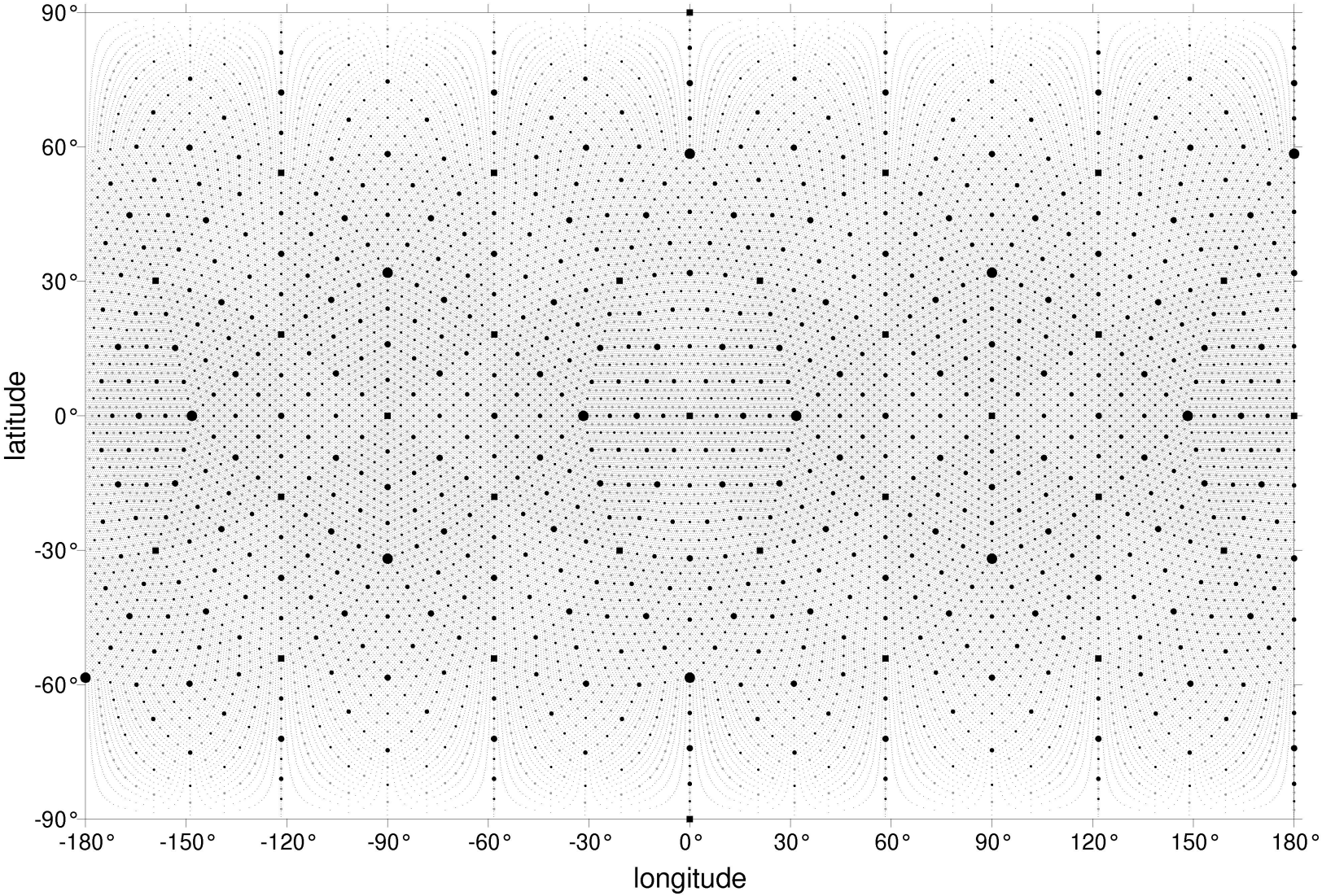

1st Iteration Step: **Comparison of the exact T with T_1**

The initial approximation $T_0 = 0$, so that we obtain T_1 from

$$A^*(T_1^{(n)}, v) = \int_{\partial\Omega} v \frac{1}{\langle \boldsymbol{s}, \boldsymbol{n} \rangle} \delta g \, dS \quad \textbf{valid for all } v \in H_n(\Omega^*) \textbf{ .}$$

The dimension of the approximation space $H_n(\Omega^*)$ is

$\boldsymbol{n} = \mathbf{163842}$ **.**

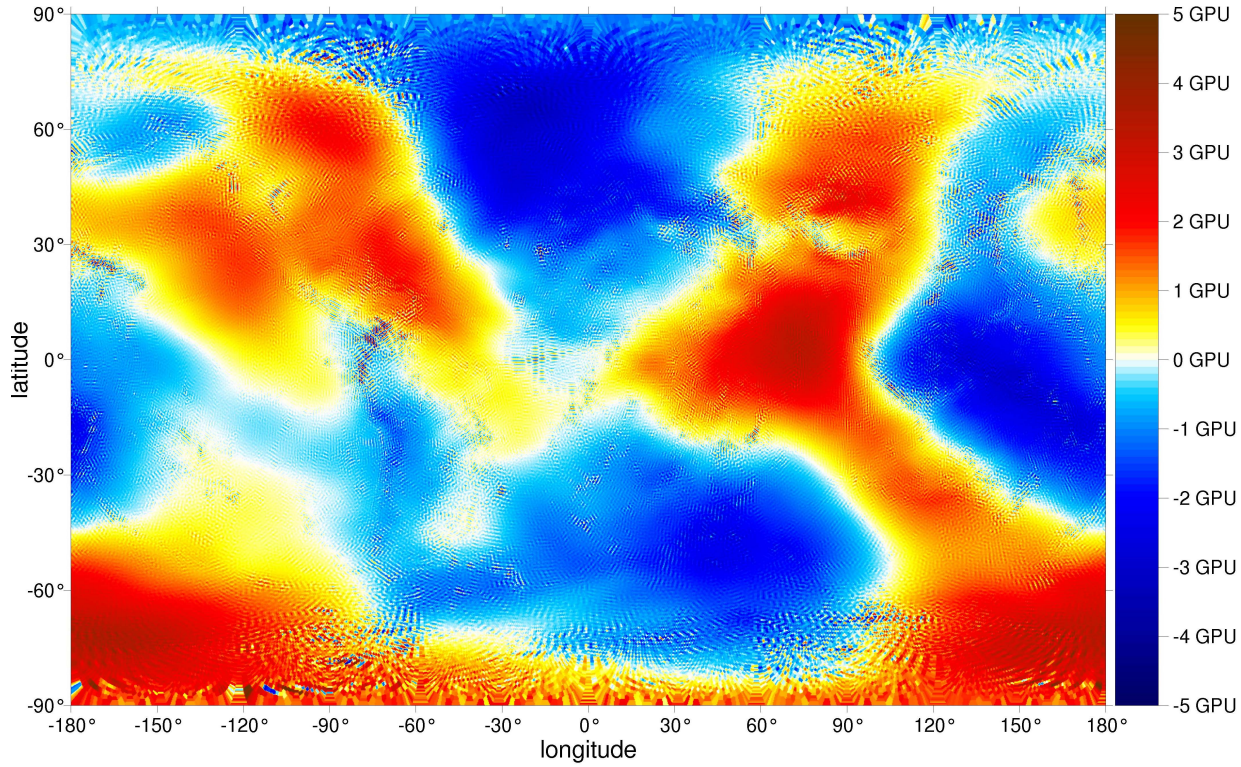

Characteristics: **min ca** $-5\,GPU$**, max ca** $5\,GPU$**, rms** $\mathbf{2.1}\,\boldsymbol{GPU}$

2nd Iteration Step: **Comparison of the exact T with T_3**

Here T_3 is defined for all $v \in H_n(\Omega^*)$ by

$$A^*(T_3^{(n)} - T_2^{(n)}, v) = \int_{\partial\Omega} v \frac{1}{\langle \boldsymbol{s}, \boldsymbol{n} \rangle} [\delta g + \langle \boldsymbol{s}, \boldsymbol{grad}\, T_2^{(n)} \rangle] \, dS \quad ,$$

The dimension of the approximation space $H_n(\Omega^*)$ is

$\boldsymbol{n} = \mathbf{163842}$ **.**

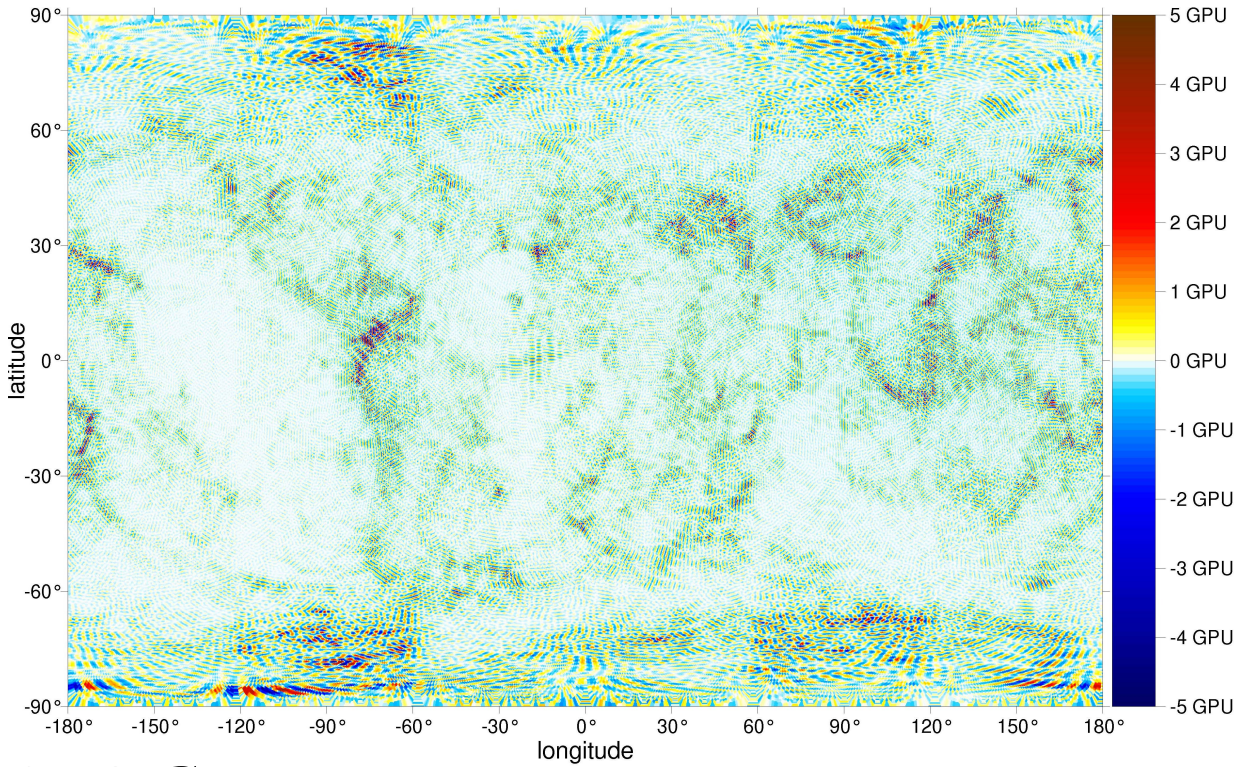

Characteristics: **rms** $\mathbf{0.38}\ GPU$ ← **!!!**

(v) *Oblique derivative effect for the ETOPO5 boundary*

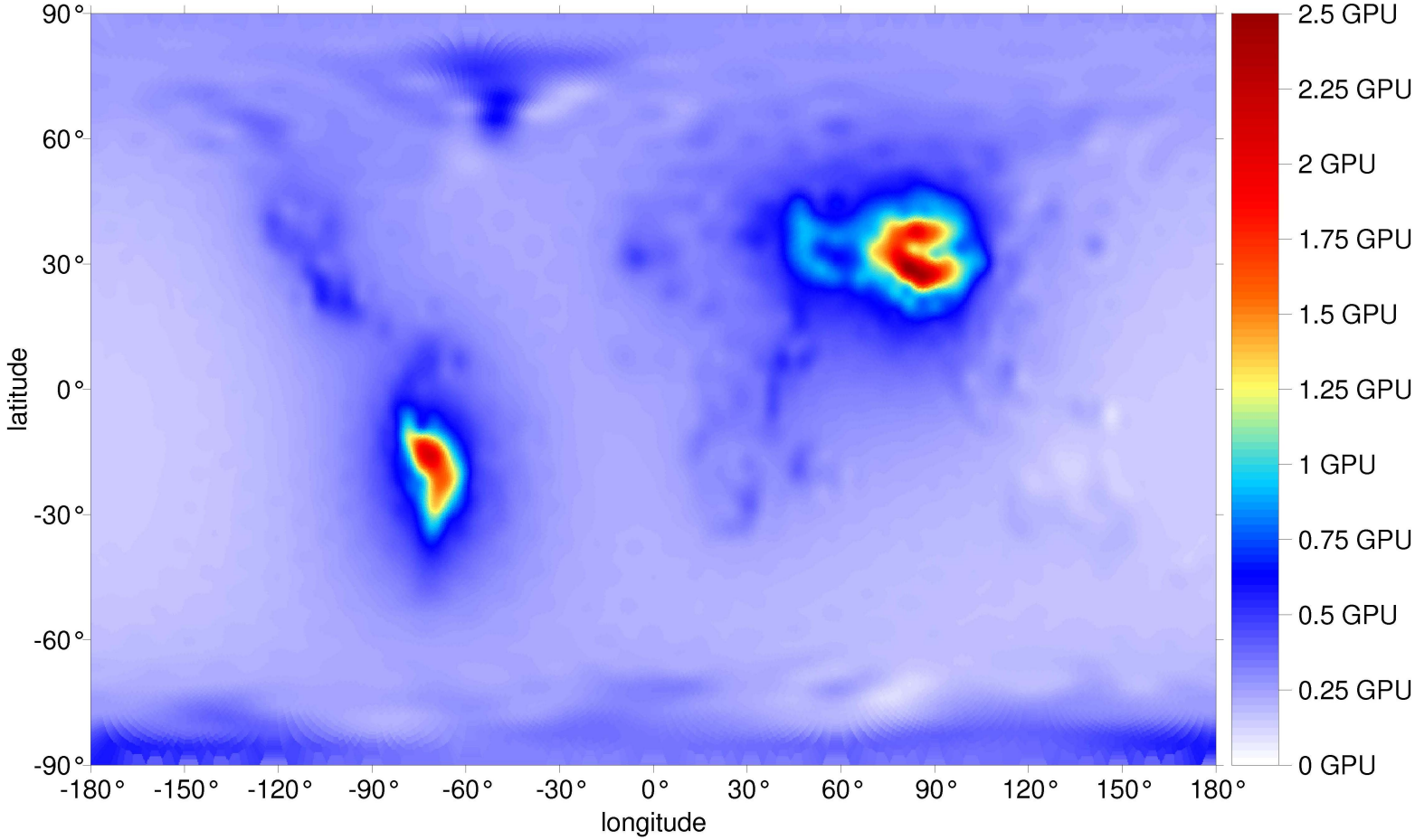

Note:

All computations done in CINECA (Consorzio Interuniversitario del Nord Est Italiano Per il Calcolo Automatico) in Bologna.

16. Reproducing Kernel

For approximation purposes the existence of a *reproducing kernel* in a particular *Hilber space* is extremely useful.

For instance in $W_2^{(1)}(\Omega)$ **consider the inner product**

$$(u,v) = A(u,v) = \sum_{i=1}^{3} \int_{\Omega} \frac{\partial u}{\partial x_i} \frac{\partial v}{\partial x_i} \, d\boldsymbol{x}$$

that induces a norm $\| u \| \equiv (u,u)^{1/2}$ ***which is equivalent to*** $\| u \|_1$

Let us try now to find a kernel $K = K(\boldsymbol{x}, \boldsymbol{y})$ **which has a *reproducing property* with respect to the inner product above, i.e.**

$$\sum_{i=1}^{3} \int_{\Omega} \frac{\partial K(\boldsymbol{x}, \boldsymbol{y})}{\partial x_i} \frac{\partial v(\boldsymbol{x})}{\partial x_i} \, d\boldsymbol{x} = v(\boldsymbol{y}) \quad \textbf{holds for all} \quad v \in W_2^{(1)}(\Omega) \, .$$

As regards $W_2^{(1)}(\Omega)$**, however, there is not too much chance to find** K **of the quality as above. This may be deduced from *Sobolev's lemma on embeddings*.**

17. Restriction to Harmonic Functions

The situation substantially changes if we consider the space $H_2^{(1)}(\Omega) \subset W_2^{(1)}(\Omega)$ of those functions from $W_2^{(1)}(\Omega)$ which are harmonic in Ω .

In case of some simple domains, we are even able to find kernels which in $H_2^{(1)}(\Omega)$ have the *reproducing property*. In $H_2^{(1)}(\Omega)$ in particular it reduces to

$$\int_{\partial\Omega} v(\boldsymbol{x}) \frac{\partial K(\boldsymbol{x},\boldsymbol{y})}{\partial n_x} d_x S = -v(\boldsymbol{y}) \quad \text{valid for all} \quad v \in H_2^{(1)}(\Omega)$$

since the kernel $K(\boldsymbol{x},\boldsymbol{y})$ must be an element of $H_2^{(1)}(\Omega)$.

4 Example – Reproducing Kernel for a Sphere

Assuming e.g. that $\Omega \equiv S_R$ and recalling the well-known integral representation of the solution of the (*exterior*) *Dirichlet problem*, we can immediately conclude that

$$\frac{\partial K(\boldsymbol{x},\boldsymbol{y})}{\partial n_x} = \frac{\partial K(\boldsymbol{x},\boldsymbol{y})}{\partial |\boldsymbol{x}|} = -\frac{1}{4\pi}\frac{\partial G(\boldsymbol{x},\boldsymbol{y})}{\partial |\boldsymbol{x}|} \quad \textbf{for} \quad |\boldsymbol{x}| = R\ ,$$

where

$$G(\boldsymbol{x},\boldsymbol{y}) = \frac{1}{|\boldsymbol{x}-\boldsymbol{y}|} - \frac{R}{|\boldsymbol{x}|}\ \frac{1}{|\bar{\boldsymbol{x}}-\boldsymbol{y}|}$$

is *Green's function*. Hence, in our spherical case we easily obtain

$$K(\boldsymbol{x},\boldsymbol{y}) = \frac{1}{4\pi R}\sum_{n=0}^{\infty}\frac{2n+1}{n+1}\rho^{n+1}P_n(\cos\psi) \quad \textbf{where} \quad \rho = \frac{R^2}{|\boldsymbol{x}||\boldsymbol{y}|}\ .$$

It is also not extremely difficult to find that

$$K(\boldsymbol{x},\boldsymbol{y}) = \frac{1}{4\pi R}\left(\frac{2\rho}{L} - \ln\frac{L+\rho-\cos\psi}{1-\cos\psi}\right)$$

where $L = \sqrt{1-2\rho\cos\psi+\rho^2}$ **,**

see e.g. *(Tscherning, 1975)*, *(Neyman, 1979)*, *(Holota, 2004, 2011)*

18. Galerkin's System and the Reproducing Kernel

Suppose now that $\boldsymbol{y}_i \in \Omega,\ i = 1\ ,\ldots,\infty$ is a sequence of points which is dense in Ω then the linear manifold

$$H = \operatorname{span}\left\{K(\boldsymbol{x}, \boldsymbol{y}_i), i = 1,\ldots,\infty\right\}$$

is densely embedded in $H_2^{(1)}(\Omega)$. Hence $K(\boldsymbol{x}, \boldsymbol{y})$ gives us a possibility to generate finite dimensional subspaces

$$H_n = \operatorname{span}\left\{K(\boldsymbol{x}, \boldsymbol{y}_i), i = 1,\ldots,n\right\} \quad \textbf{in} \quad H_2^{(1)}(\Omega)$$

such that $H_n \subseteq H_{n+1}$ and $\lim\limits_{n \to \infty} \operatorname{dist}(v, H_n) = 0$ for all $v \in H_2^{(1)}$, i.e.,

$$\lim_{n \to \infty} H_n = H_2^{(1)} \ .$$

This is important since it enables us to approximate the solution by means of the linear combinations

$$u_n = \sum_{j=1}^{n} c_j^{(n)} v_j \quad \textbf{where} \quad v_j(\boldsymbol{x}) = K(\boldsymbol{x}, \boldsymbol{y}_j) \ .$$

In addition, in *Galerkin's system*

$$\sum_{j=1}^{n} c_j^{(n)} A(v_j, v_k) = \int_{\partial\Omega} v_k \, f \, dS \ , \qquad k = 1, \ldots, n$$

the elements $A(v_j, v_k)$ may be immediately expressed by

$$A(v_j, v_k) = K(\boldsymbol{y}_j, \boldsymbol{y}_k) \qquad (\ !!!\ )$$

***in view of the reproducing property of the kernel*.**

19. Reproducing Kernel for an Ellipsoid

The possibility to express $A(v_j, v_k)$ by means of $K(\boldsymbol{x}, \boldsymbol{y})$ leads us to an attempt to construct a kernel $K_{ell}(\boldsymbol{x}, \boldsymbol{y})$ which has the reproducing property also in case that Ω is the exterior Ω_{ell} of an oblate ellipsoid of revolution of semi-axes a and b, $a \geq b$.

Naturally, we will use ellipsoidal coordinates u, β, λ. They are related to x_1, x_2, x_3 by the equations

$$x_1 = \sqrt{u^2 + E^2}\cos\beta\cos\lambda\ , \quad x_2 = \sqrt{u^2 + E^2}\cos\beta\sin\lambda\ , \quad x_3 = u\sin\beta$$

where $E = \sqrt{a^2 - b^2}$.

***Note*. In the coordinates u, β, λ the boundary $\partial\Omega_{ell}$ of Ω_{ell} is defined by $u = b$.**

In analogy to the spherical case we now have

$$\int_{\partial\Omega_{ell}} v(\boldsymbol{x}) \frac{\partial K_{ell}(\boldsymbol{x},\boldsymbol{y})}{\partial n_x} d_x S = -v(\boldsymbol{y})$$

and subsequently also

$$\frac{\partial K_{ell}(\boldsymbol{x},\boldsymbol{y})}{\partial n_x} = -\frac{1}{4\pi} \frac{\partial G_{ell}(\boldsymbol{x},\boldsymbol{y})}{\partial n_x} \qquad \textbf{for} \quad u_x = b \qquad \textbf{(3)}$$

where $G_{ell}(\boldsymbol{x},\boldsymbol{y})$ **is** ***Green's function*** **related to** ***Dirichlet's problem*** **formulated for** Ω_{ell}**.**

Referring to *(Holota, IAG Symposia, 2004)* and *(Holota, Studia geophysica et geodaetica, 2011)*, we can deduce from *Eq. (3)* that

$$K_{ell}(\boldsymbol{x},\boldsymbol{y}) = \frac{1}{4\pi b}\sum_{n=0}^{\infty}(2n+1)\Big[K_{n0xy}P_n(\sin\beta_x)P_n(\sin\beta_y) + \\ + 2\sum_{m=1}^{n}\frac{(n-m)!}{(n+m)!}K_{nmxy}\,P_{nm}(\sin\beta_x)P_{nm}(\sin\beta_y)\cos m(\lambda_x-\lambda_y)\Big] \qquad \textbf{(4)}$$

with

$$K_{nmxy} = \frac{iEb}{a^2}\frac{Q_{nm}(z_x)}{Q_{nm}(z_0)}\frac{Q_{nm}(z_y)}{Q_{nm}(z_0)}\left[\frac{dQ_{nm}(z_0)}{dz}\Big/Q_{nm}(z_0)\right]^{-1} \qquad \textbf{(5)}$$

where P_{nm} and Q_{nm} are *Legendre's functions* of the 1st and the 2nd kind, while

$$z_x = \frac{iu_x}{E}\,,\quad z_y = \frac{iu_y}{E}\,,\quad z_0 = \frac{ib}{E}\quad \textbf{and}\quad i = \sqrt{-1}.$$

Recall **also that** Q_{nm} **can be expressed as**

$$Q_{nm}(z)=(-1)^m\frac{2^n n!(n+m)!}{(2n+1)!}(z^2-1)^{-\frac{n+1}{2}}F\left(\frac{n+m+1}{2},\frac{n-m+1}{2},\frac{2n+3}{2};\frac{1}{1-z^2}\right)$$

where F **is a *hypergeometric function* and that, passing to *hypergeometric series*,**

$$F_z=F\left(a,b,c;\frac{1}{1-z^2}\right)=1+\sum_{n=1}^{\infty}\frac{(a)_n(b)_n}{(c)_n\,n!}\left(\frac{1}{1-z^2}\right)^n$$

with

$$(a)_n=a(a+1)\ldots(a+n-1),\ \ n=1,2,3\ldots$$

$$(b)_n=b(b+1)\ldots(b+n-1),\ \ n=1,2,3\ldots$$

$$(c)_n=c(c+1)\ldots(c+n-1),\ \ n=1,2,3\ldots$$

Note. **The series converges which may be directly verified by using e.g. *d'Alembert convergence criterion*.**

In *Fig. 1* the kernel $K_{ell}(\boldsymbol{x},\boldsymbol{y})$ is illustrated for two configurations and an ellipsoid of parameters given by the GRS80 system.

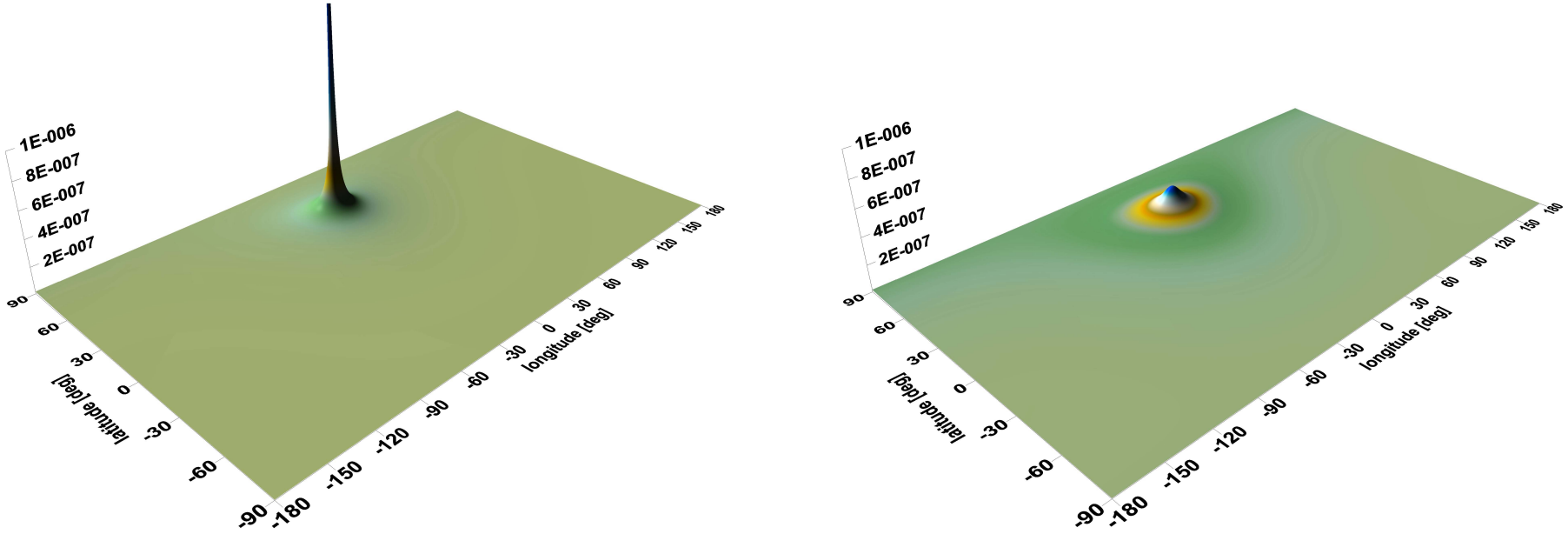

Figure 1. Kernel function $K_{ell}(\boldsymbol{x},\boldsymbol{y})$ for $\beta_y = 45°$ (north) and $\lambda_y = 0°$:
(Left) $u_y = 1.001b$, (Right) $u_y = 1.1b$.
Note that $\boldsymbol{x}$ is the moving point with $u_x = b$.

20. Computational Aspects - Approximation of the Kernel

The implementation of

$$K_{ell}(\boldsymbol{x},\boldsymbol{y})$$

on the basis of *Eqs. (4)* and *(5)* is feasible, but extremely demanding in case that all the entries of *Galerkin's matrix* and right sides in *Galerkin's system* have to be computed, e.g. in *high resolution modelling of the solution*.

***This motivates* studies leading to (analytical) *summation of the series representing the kernel*. In solving this problem we used some approximations.**

After elementary modifications we have

$$F_z = F_{z_0} + \frac{ab}{c}\left(\frac{1}{1-z^2} - \frac{1}{1-z_0^2}\right) + \frac{a(a+1)b(b+1)}{2c(c+1)}\left[\left(\frac{1}{1-z^2}\right)^2 - \left(\frac{1}{1-z_0^2}\right)^2\right] + \cdots$$

Thus, e.g., in a $20km$ layer close above the ellipsoid

$$\frac{1}{1-z^2}-\frac{1}{1-z_0^2} \le e^4 = 0,000046 \quad \textbf{and}$$

$$\left(\frac{1}{1-z^2}\right)^2-\left(\frac{1}{1-z_0^2}\right)^2 \le 2e^6 = 0,0000006 \quad \textbf{etc.}$$

In the sequel, therefore, considering these estimates, we put

$$\frac{Q_{nm}(z_x)}{Q_{nm}(z_0)}\frac{Q_{nm}(z_y)}{Q_{nm}(z_0)} \approx \rho^{n+1} \quad \textbf{where} \quad \rho = \frac{a^2}{\sqrt{u_x^2+E^2}\sqrt{u_y^2+E^2}}$$

Similarly recalling that $\dfrac{dQ_{nm}}{dz} = \dfrac{(n+1)\,z}{1-z^2}Q_{nm} - \dfrac{n-m+1}{1-z^2}Q_{n+1,m}$

and putting $\dfrac{Q_{n+1,m}(z_0)}{Q_{nm}(z_0)} \approx \dfrac{n+m+1}{2n+3}\dfrac{E}{ia}$ **we arrive at**

$$\frac{1}{Q_{nm}(z_0)}\frac{dQ_{nm}(z_0)}{dz} \approx i\frac{Eb}{a^2}(n+1)\left[1+\frac{E^2}{ab}\frac{(n+1)^2-m^2}{(n+1)(2n+3)}\right]$$

Hence

$$K_{nmxy} \approx \rho^{n+1}\kappa_{nm} \quad \textbf{with} \quad \kappa_{nm} = \frac{1}{n+1}\left[1-\frac{E^2}{ab}\frac{(n+1)^2-m^2}{(n+1)(2n+3)}\right] \qquad \textbf{(6)}$$

Below κ_{nm} is compared with κ_{nmxy} (exact), i.e.

$$\kappa_{nmxy} = \rho^{-(n+1)}K_{nmxy}$$

computed numerically from *Eqs. (4)* and *(5)*.

The difference

$$\delta\kappa_{nmxy} = \kappa_{nmxy} - \kappa_{nm}$$

and its relative counterpart

$$\delta^{(rel)}\kappa_{nmxy} = \delta\kappa_{nmxy} / \kappa_{nmxy}$$

are plotted in *Fig. 2*.

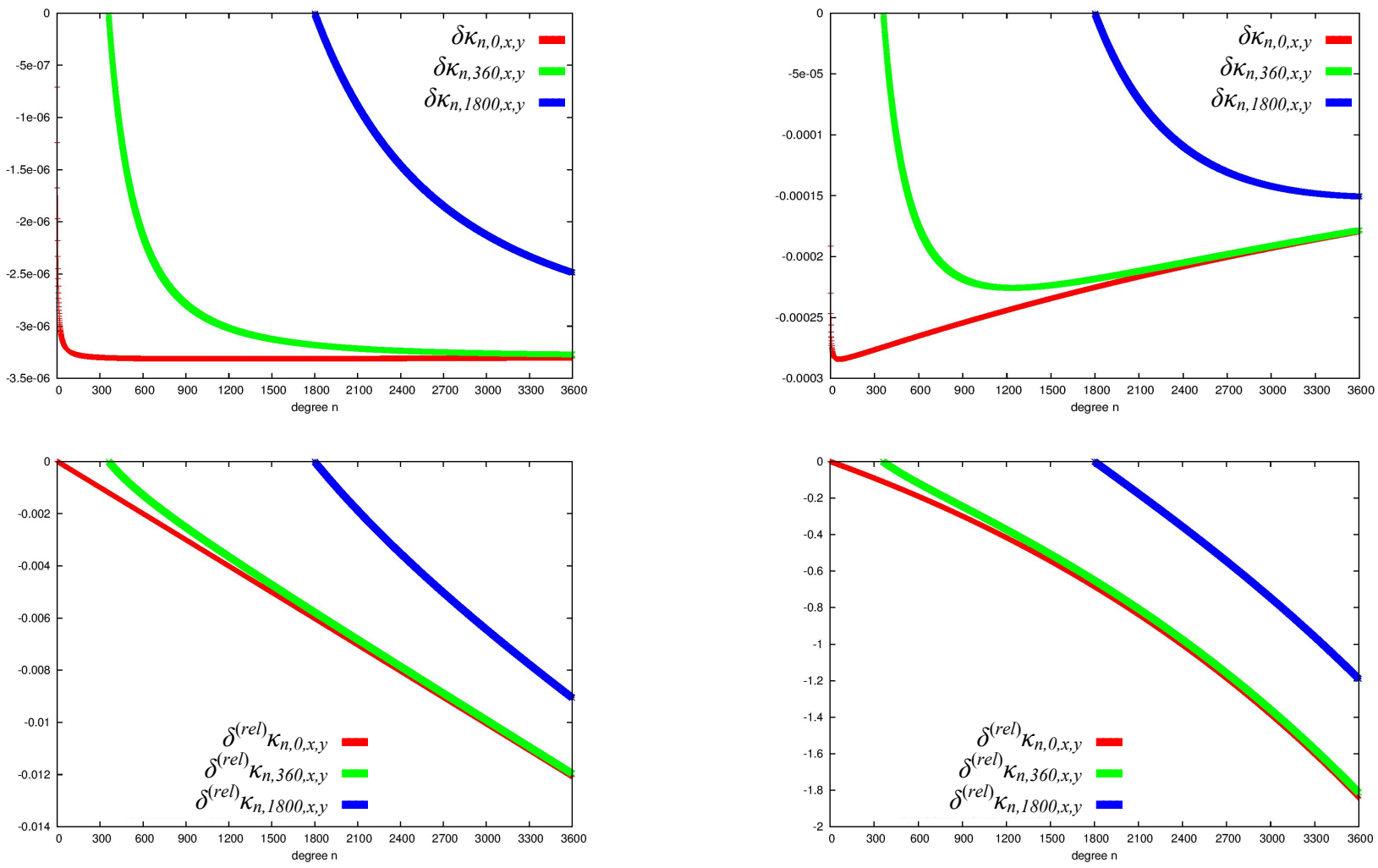

Figure 2. (Above) absolute difference $\delta\kappa_{nmxy}$, (Below) relative difference $\delta^{(rel)}\kappa_{nmxy}$:

(Left) $u_x = b$ and $u_y = 1.001b$, (Right) $u_x = b$ and $u_y = 1.1b$

Return **now to** $K_{ell}(\boldsymbol{x},\boldsymbol{y})$ **with coefficients** K_{nmxy} **given by** ***Eq. (6)*****.**

Denoting by ψ **the angular distance of points** (β_x,λ_y) **and** (β_y,λ_y) **on a sphere, when** β **and** λ **are interpreted as spherical latitude and longitude, respectively and using the well-known** ***Legendre's addition theorem*****, we can write**

$$\tilde{K}_{ell}(\boldsymbol{x},\boldsymbol{y}) = \frac{1}{4\pi b}K^{(1)}(\boldsymbol{x},\boldsymbol{y}) - \frac{E}{4\pi ab^2}K^{(2)}(\boldsymbol{x},\boldsymbol{y}) + \frac{E}{4\pi ab^2}K^{(3)}(\boldsymbol{x},\boldsymbol{y}) \quad \textbf{(7)}$$

with

$$K^{(1)}(\boldsymbol{x},\boldsymbol{y}) = \sum_{n=0}^{\infty}\frac{2n+1}{n+1}\rho^{n+1}P_n(\cos\psi)$$

$$K^{(2)}(\boldsymbol{x},\boldsymbol{y}) = \sum_{n=0}^{\infty}\frac{2n+1}{2n+3}\rho^{n+1}P_n(\cos\psi) \quad \textbf{and}$$

$$K^{(3)}(\boldsymbol{x},\boldsymbol{y}) = -\sum_{n=1}^{\infty}\frac{2n+1}{(n+1)^2(2n+3)}\rho^{n+1}\frac{\partial^2 P_n(\cos\psi)}{\partial\lambda^2}$$

for the last term also ***(Holota, 2003)*** **has been used.**

20.1. Summation of $K^{(1)}$

We first split the term into two parts

$$K^{(1)}(\boldsymbol{x},\boldsymbol{y}) = 2\sum_{n=0}^{\infty}\rho^{n+1}P_n(\cos\psi) - \sum_{n=0}^{\infty}\frac{1}{n+1}\rho^{n+1}P_n(\cos\psi)$$

Then, recalling

$$\sum_{n=0}^{\infty}\rho^{n}P_n(\cos\psi) = \frac{1}{L} \quad \textbf{where} \quad L = \sqrt{1-2\rho\cos\psi+\rho^2}$$

we after some manipulation and integration arrive at

$$K^{(1)}(\boldsymbol{x},\boldsymbol{y}) = \frac{2\rho}{L} - \ln\frac{L+\rho-\cos\psi}{1-\cos\psi}$$

see e.g. *(Tscherning, 1975)*, *(Neyman, 1979)*, *(Holota, 2004, 2011)*

20.2. Summation of $K^{(2)}$ – Elliptic Integrals

One can easily verify that

$$K^{(2)}(\boldsymbol{x},\boldsymbol{y}) = \sum_{n=0}^{\infty} \rho^{n+1} P_n(\cos\psi) - 2\sum_{n=0}^{\infty} \frac{1}{n+3}\, \rho^{n+1} P_n(\cos\psi)$$

The *summation of the 2nd term is more complex*. Putting

$$S = \sum_{n=0}^{\infty} \frac{1}{n+3}\, \rho^{n+1} P_n(\cos\psi)\ ,$$ **we deduce that** $$\frac{dS}{d\rho} + \frac{1}{2\rho} S = \frac{1}{2L}$$

***This is an elementary differential equation*. Its general solution is**

$$S = \frac{C(\psi)}{\sqrt{\rho}} + \frac{1}{2\sqrt{\rho}} \int \frac{\sqrt{\rho}}{L}\, d\rho\ ,\quad C(\psi)$$ **is an arbitrary function of** ψ

while *2nd term* is an *elliptic integral*.

To apply a standard approach for its computation we express it in a *trigonometric form*. *For this purpose we replace*

ρ ***by a new variable*** $\varphi \in \langle 0, \frac{\pi}{2} \rangle$ ***according to*** $\rho = \tan^2 \frac{\varphi}{2}$

After some algebra we arrive at

$$S = C(\psi)\left(\tan\frac{\varphi}{2}\right)^{-1} + \sqrt{1-k^2\sin^2\varphi} + \frac{1}{2}\left(\tan\frac{\varphi}{2}\right)^{-1}\left[\mathcal{F}(k,\varphi) - 2\mathcal{E}(k,\varphi)\right]$$

where

$$k^2 = \cos^2\frac{\psi}{2} \quad ,$$

$$\mathcal{F}(k,\varphi) = \int_0^{\varphi} \frac{d\varphi}{\sqrt{1-k^2\sin^2\varphi}} \quad \textbf{and} \quad \mathcal{E}(k,\varphi) = \int_0^{\varphi} \sqrt{1-k^2\sin^2\varphi}\, d\varphi$$

are the *Legendre (incomplete) elliptic integrals of the first and the second kind*. Moreover, comparing the left and the right hand side for $\rho = 0$ (i.e. $\varphi = 0$), we obtain $C(\psi) = 0$ and subsequently

$$K^{(2)}(\boldsymbol{x},\boldsymbol{y}) = \frac{\rho}{L} - 2\sqrt{1-k^2\sin^2\varphi} - \left(\tan\frac{\varphi}{2}\right)^{-1}\left[\mathcal{F}(k,\varphi) - 2\mathcal{E}(k,\varphi)\right]$$

20.3. Summation of $K^{(3)}$ – Elliptic Integrals

The term $K^{(3)}$, i.e.

$$K^{(3)}(\boldsymbol{x},\boldsymbol{y}) = -\sum_{n=1}^{\infty} \frac{2n+1}{(n+1)^2(2n+3)} \rho^{n+1} \frac{\partial^2 P_n(\cos\psi)}{\partial^2 \lambda}$$

requires also a special treatment. First we compute

$$\frac{\partial^2 P_n(\cos\psi)}{\partial \lambda^2} = \frac{d^2 P_n(\cos\psi)}{d(\cos\psi)^2} \left(\frac{\partial \cos\psi}{\partial \lambda} \right)^2 + \frac{dP_n(\cos\psi)}{d\cos\psi} \frac{\partial^2 \cos\psi}{\partial \lambda^2}$$

where

$$\left(\frac{\partial \cos\psi}{\partial \lambda} \right)^2 = \cos^2\beta_x \cos^2\beta_y \sin^2(\lambda_x - \lambda_y) = \sin^2\psi \sin^2\alpha_{xy} \cos^2\beta_y$$

$$\frac{\partial^2 \cos\psi}{\partial \lambda^2} = -\cos\beta_x \cos\beta_y \cos(\lambda_x - \lambda_y) = \sin\beta_x \sin\beta_y - \cos\psi$$

Then, using *Legendre's differential equation*

$$\frac{d^2 P_n(\cos\psi)}{d(\cos\psi)^2} - \frac{2\cos\psi}{\sin^2\psi}\cdot\frac{dP_n(\cos\psi)}{d\cos\psi} + \frac{n(n+1)}{\sin^2\psi}P_n(\cos\psi) = 0$$

we obtain

$$\frac{\partial^2 P_n(\cos\psi)}{\partial\lambda^2} = (*)\frac{dP_n(\cos\psi)}{d\cos\psi} - \frac{n(n+1)}{\sin^2\psi}\left(\frac{\partial\cos\psi}{\partial\lambda}\right)^2 P_n(\cos\psi)$$

with

$$(*) = \frac{\partial^2\cos\psi}{\partial\lambda^2} + \frac{2\cos\psi}{\sin^2\psi}\left(\frac{\partial\cos\psi}{\partial\lambda}\right)^2 = \sin\beta_x\sin\beta_y - (1-2\sin^2\alpha_{xy}\cos^2\beta_y)\cos\psi$$

Recalling finally that

$$\frac{dP_n(\cos\psi)}{d\cos\psi} = \frac{n+1}{\sin^2\psi}\left[\cos\psi P_n(\cos\psi) - P_{n+1}(\cos\psi)\right]$$

we get

$$K^{(3)}(\boldsymbol{x},\boldsymbol{y}) = S_1 \sin^2\alpha_{xy} \cos^2\beta_y - (*)\, S_2$$

with

$$S_1 = \sum_{n=1}^{\infty} \frac{n(2n+1)}{(n+1)(2n+3)} \rho^{n+1} P_n(\cos\psi)$$

and

$$S_2 = \frac{1}{\sin^2\psi}\left[S_{21}\cos\psi - S_{22}\right]$$

where

$$S_{21} = \sum_{n=1}^{\infty} \frac{2n+1}{(n+1)(2n+3)} \rho^{n+1} P_n(\cos\psi)$$

and

$$S_{22} = \sum_{n=2}^{\infty} \frac{2n-1}{n(2n+1)} \rho^{n} P_n(\cos\psi)$$

***Note*. In the second term we somewhat adjusted the index n.**

- **In the sequel *we approach the summation in* S_1 *first*. We can split it as follows**

$$S_1 = -K^{(1)}(\boldsymbol{x},\boldsymbol{y}) + 3K^{(2)}(\boldsymbol{x},\boldsymbol{y})$$

so that, recalling Sec. (7.1) and (7.2),

$$S_1 = \frac{\rho}{L} + \ln\frac{L+\rho-\cos\psi}{1-\cos\psi} - 6\sqrt{1-k^2\sin^2\varphi} - 3\left(\tan\frac{\varphi}{2}\right)^{-1}\left[\mathcal{F}(k,\varphi) - 2\mathcal{E}(k,\varphi)\right]$$

- ***Now we treat*** S_2 **and will start with the** S_{21}**- term. One can easily verify that**

$$S_{21} = -\frac{\rho}{3} + K^{(1)}(\boldsymbol{x},\boldsymbol{y}) - 2K^{(2)}(\boldsymbol{x},\boldsymbol{y})$$

thus

$$S_{21} = -\frac{\rho}{3} - \ln\frac{L+\rho-\cos\psi}{1-\cos\psi} + 4\sqrt{1-k^2\sin^2\varphi} + 2\left(\tan\frac{\varphi}{2}\right)^{-1}\left[\mathcal{F}(k,\varphi) - 2\mathcal{E}(k,\varphi)\right]$$

- ***Finally, we have to discuss*** **the S_{22}- term. We split it again, so that**

$$S_{22} = -4 - \frac{\rho}{3} - \sum_{n=1}^{\infty} \frac{1}{n} \rho^n P_n(\cos\psi) + 4 \sum_{n=0}^{\infty} \frac{1}{2n+1} \rho^n P_n(\cos\psi)$$

On the right hand side for the *3rd* term we derive that

$$\sum_{n=1}^{\infty} \frac{1}{n} \rho^n P_n(\cos\psi) = -\ln \frac{L+1-\rho\cos\psi}{2}$$

and with the aid of the *elliptic integrals of the first kind* we obtain

$$\sum_{n=0}^{\infty} \frac{1}{2n+1} \rho^n P_n(\cos\psi) = \frac{1}{2}\left(\tan\frac{\varphi}{2}\right)^{-1} \mathcal{F}(k,\varphi).$$

Hence

$$S_{22} = -4 - \frac{\rho}{3}\cos\psi + \ln \frac{L+1-\rho\cos\psi}{2} + 2\left(\tan\frac{\varphi}{2}\right)^{-1} \mathcal{F}(k,\varphi)$$

21. Approximation Computation of the Kernel

In this section $\tilde{K}_{ell}(\boldsymbol{x},\boldsymbol{y})$ computed on the basis of *Eq. (7)* and formulas derived in sections 20.1 - 20.3 is compared with $K_{ell}(\boldsymbol{x},\boldsymbol{y})$ (exact) computed from *Eqs. (4)* and *(5)*.

For the ellipsoid of parameters given by the GRS80 the difference is illustrated in the figures below. *On the left side* (blue) they show

$$\delta K(\boldsymbol{x},\boldsymbol{y}) = \left[K_{ell}(\boldsymbol{x},\boldsymbol{y}) - \frac{1}{4\pi b} K^{(1)}(\boldsymbol{x},\boldsymbol{y}) \right] K_{ell}^{-1}(\boldsymbol{x},\boldsymbol{y})$$

while the *right side* (green) illustrates

$$\delta \tilde{K}(\boldsymbol{x},\boldsymbol{y}) = \left[K_{ell}(\boldsymbol{x},\boldsymbol{y}) - \tilde{K}_{ell}(\boldsymbol{x},\boldsymbol{y}) \right] K_{ell}^{-1}(\boldsymbol{x},\boldsymbol{y})$$

***The values are in ppm* (i.e. 10^{-6}).**

In constructing the figures $\boldsymbol{x}$ was taken for the *moving point* with $u_x = b$ and $\boldsymbol{y}$ for the *computation point* with $\beta = 0^\circ$ and $\lambda = 0^\circ$. Moreover, three values of u_y were considered.

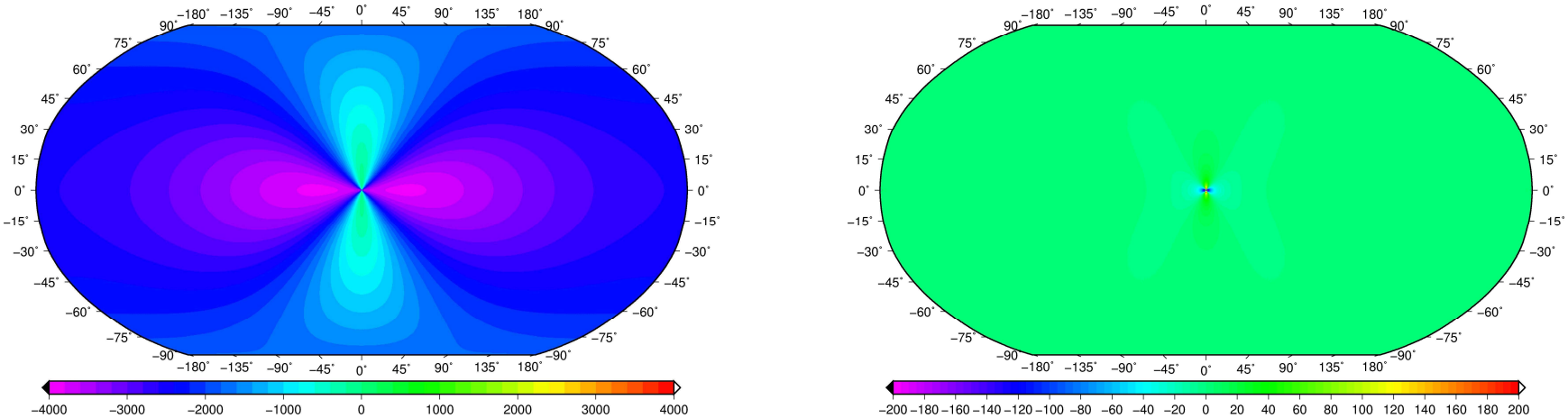

Figure 3a. (Left) $\delta K(\boldsymbol{x},\boldsymbol{y})$ and (Right) $\delta\tilde{K}(\boldsymbol{x},\boldsymbol{y})$ for: $u_y = 1.001b$, i.e. $\boldsymbol{y}$ ca $6.3\,km$ above the ellipsoid.

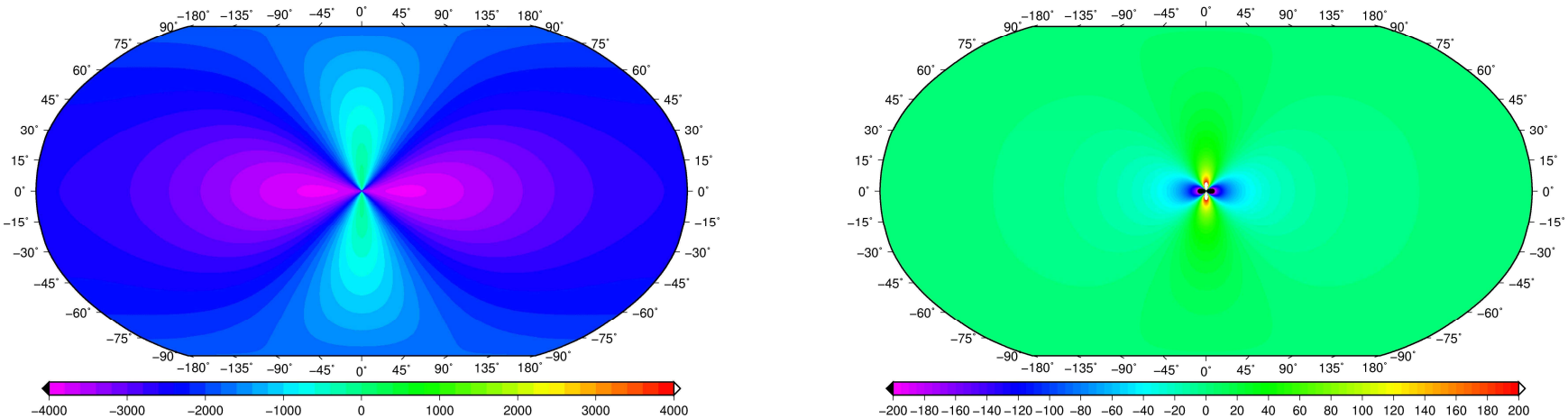

Figure 3b. (Left) $\delta K(\boldsymbol{x},\boldsymbol{y})$ and (Right) $\delta\tilde{K}(\boldsymbol{x},\boldsymbol{y})$ for: $u_y = 1.005b$, i.e. $\boldsymbol{y}$ ca $32\,km$ above the ellipsoid.

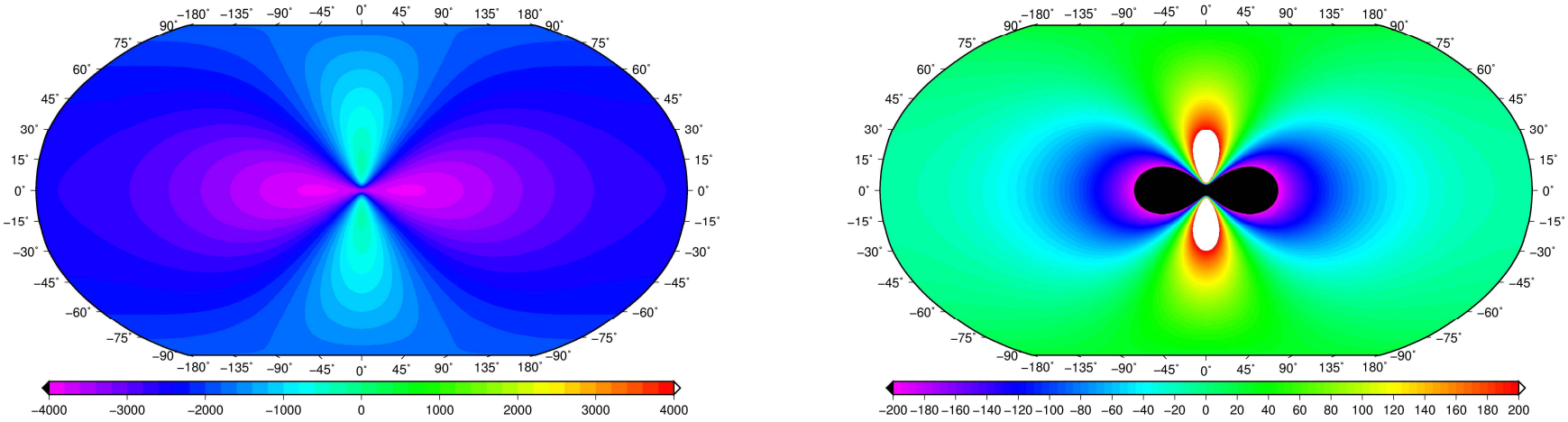

Figure 3c. (Left) $\delta K(\boldsymbol{x},\boldsymbol{y})$ and (Right) $\delta\tilde{K}(\boldsymbol{x},\boldsymbol{y})$ for: $u_y = 1.04b$, i.e. $\boldsymbol{y}$ ca $260\,km$ above the ellipsoid.

The figures indicate that there are good reasons to expect that $\tilde{K}_{ell}(\boldsymbol{x},\boldsymbol{y})$ will be an efficient tool for solving potential problems in gravity field studies, e.g., computing the disturbing potential.

The problems mentioned above were investigated and also added extensive numerical tests in *(Holota and Nesvadba 2007, 2012)* and *(Nesvadba et al. 2007)*.

22. Integral Kernels in Data Combinations

It is well-known in physical geodesy that the solution of *Stokes' problem* is given by

$$T(x) = \frac{R}{r} T_0 + \left(\frac{R}{r}\right)^2 T_1 + R \sum_{n=2}^{\infty} \left(\frac{R}{r}\right)^{n+1} \frac{1}{n-1} \Delta g_n \quad , \qquad r = |\boldsymbol{x}|$$

and that for $r = R$ and some assumptions concerning T_0 and T_1,

$$T = \frac{R}{4\pi} \int_\sigma S(\psi) \Delta g \, d\sigma \quad \text{with} \quad S(\psi) = \sum_{n=2}^{\infty} \frac{2n+1}{n-1} P_n(\cos\psi)$$

representing the famous *Stokes kernel*.

Similarly, when using *gravity disturbances* we have

$$T(x) = R \sum_{n=0}^{\infty} \left(\frac{R}{r}\right)^{n+1} \frac{1}{n+1} \delta g_n$$

$$T = \frac{R}{4\pi} \int_\sigma K(\psi) \delta g \, d\sigma \quad \text{and} \quad K(\psi) = \sum_{n=0}^{\infty} \frac{2n+1}{n+1} P_n(\cos\psi)$$

that sometimes is called *Neumann-Koch function*.

Naturally, the use of *global gravity field models* stimulates some modification of this approach. E.g. we put

$$T(x)=\frac{R}{r}T_0+\left(\frac{R}{r}\right)^2 T_1+\cdots+\left(\frac{R}{r}\right)^N T_{N-1}+R\sum_{n=N}^{\infty}\left(\frac{R}{r}\right)^{n+1}\frac{1}{n-1}\Delta g_n$$

or

$$T(x)=\frac{R}{r}T_0+\left(\frac{R}{r}\right)^2 T_1+\cdots+\left(\frac{R}{r}\right)^N T_{N-1}+R\sum_{n=N}^{\infty}\left(\frac{R}{r}\right)^{n+1}\frac{1}{n+1}\delta g_n$$

compute gravity anomalies Δg or disturbances δg with respect to an adopted model, put $T_n=0$ for $n=0,1,2,\ldots,N-1$ and subsequently work with the *reduced Stokes or Neumann-Koch kernel*

$$S_{red}^{(N)}(\psi)=\sum_{n=N}^{\infty}\frac{2n+1}{n-1}P_n(\cos\psi) \quad \textbf{or} \quad K_{red}^{(N)}(\psi)=\sum_{n=N}^{\infty}\frac{2n+1}{n+1}P_n(\cos\psi)$$

Graphically the kernels are illustrated in the figures that follow.

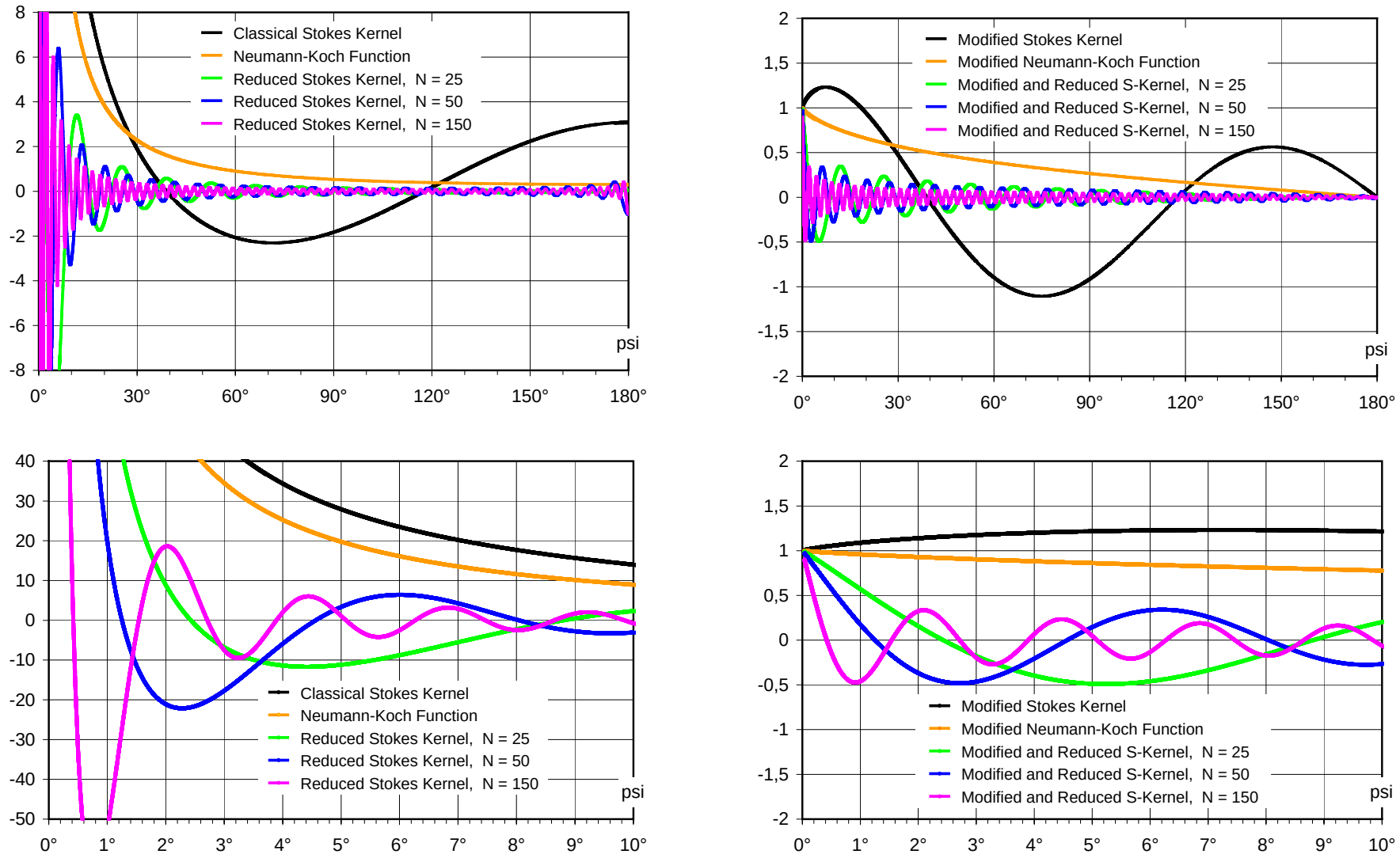

The approach as above is straightforward, but not the only concept possible.

Data from the *GOCE* mission and *terrestrial gravity measurements* are *two different sources of information*. Their combination has an essential tie to potential theory.

Within the space-wise approach we will discuss the use of gravity field information contained *in satellite-only models* or *alternatively in GOCE gradiometric data* in common *with terrestrial gravity measurements*

In the sequel Ω means a solution domain bounded by two surfaces. With some simplification we suppose that Ω is bounded by two spheres of radius R_i and R_e, $R_i < R_e$.

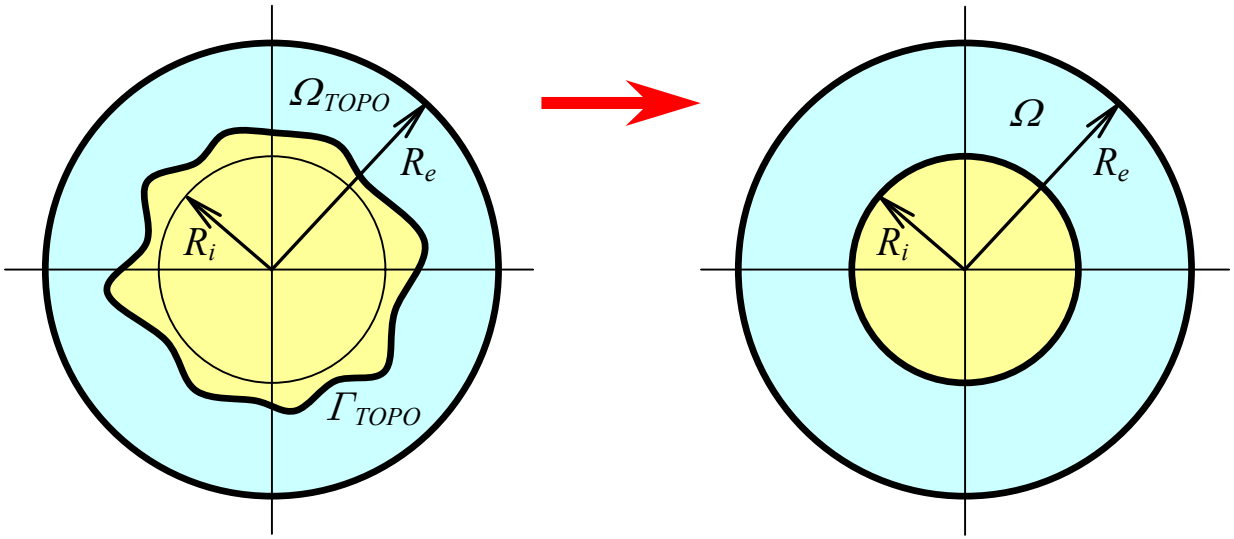

23. Potential Problems

We consider first *gravimetry and a satellite-only model*, thus the following problem

$$\Delta T = 0 \quad \text{in} \quad \Omega$$

$$\frac{\partial T}{\partial r} + \frac{2}{R_i} T = -\Delta g \quad \text{for} \quad r = R_i \qquad \text{and} \qquad T = t \quad \text{for} \quad r = R_e$$

Here: Δg **is *the gravity anomaly***

t **means the *input from an available satellite-only model***

The domain Ω **is bounded.** $\Rightarrow$ **Therefore, the solution** $T = (r, \varphi, \lambda)$**, we are looking for, has generally the form**

$$T = T^{(i)} + T^{(e)} \tag{3}$$

$$T^{(i)} = \sum_{n=0}^{\infty} \left(\frac{R_i}{r} \right)^{n+1} T_n^{(i)}(\varphi, \lambda) \qquad \text{and} \qquad T^{(e)} = \sum_{n=0}^{\infty} \left(\frac{r}{R_e} \right)^{n} T_n^{(e)}(\varphi, \lambda)$$

where $T_n^{(i)}$ **and** $T_n^{(e)}$ **are the *surface spherical harmonics*.**

Using the orthogonality of spherical harmonics, we obtain a *linear system* for $T_n^{(i)}$ and $T_n^{(e)}$, that for and individual n *yields*

$$T_n^{(i)} = \frac{R_i \, \Delta g_n \; + \; (n+2) \, q^n t_n}{D_n^{(p)}} \qquad \textbf{(4a)}$$

and

$$T_n^{(e)} = -\frac{R_i \, q^{n+1} \Delta g_n - (n-1) \, t_n}{D_n^{(p)}} \qquad \textbf{(4b)}$$

where

$D_n^{(p)} = (n+2)(1+q^{2n+1}) - 3$ ***is the determinant,*** $q = R_i / R_e$

while Δg_n and t_n are *surface spherical harmonics* in the developments of Δg and t, respectively, i.e. in

$$\Delta g(\varphi,\lambda) = \Sigma_{n=0}^{\infty} \Delta g_n(\varphi,\lambda) \qquad \textbf{and} \qquad t(\varphi,\lambda) = \Sigma_{n=0}^{\infty} t_n(\varphi,\lambda).$$

Similarly for *gravimetry and gradiometry* the problem is to find T such that

$$\Delta T = 0 \quad \text{in} \quad \Omega$$

$$\frac{\partial T}{\partial r} + \frac{2}{R_i} T = -\Delta g \quad \text{for} \quad r = R_i \quad \text{and} \quad \frac{\partial^2 T}{\partial r^2} = G \quad \text{for} \quad r = R_e$$

***The input from satellite gradiometry* is symbolized by $G(\varphi,\lambda) = \Sigma_{n=0}^{\infty} G_n(\varphi,\lambda)$, where G_n are *the respective surface spherical harmonics*.**

Using the orthogonality of spherical harmonics again, we for any individual n arrive at

$$T_n^{(i)} = \left[R_i n(n-1)\Delta g_n + R_e^2 (n+2) q^n G_n \right] \frac{1}{D_n^{(g)}}$$

$$T_n^{(e)} = -\left[R_i (n+1)(n+2) q^{n+1} \Delta g_n - R_e^2 (n-1) G_n \right] \frac{1}{D_n^{(g)}}$$

where $D_n^{(g)} = n(n-1)^2 + (n+1)(n+2)^2 q^{2n+1}$.

24. Compatibility

In both the cases we found a solution, which is harmonic in Ω. The problem, however, is that the continuation of T for $r > R_e$ *need not be regular at infinity*, i.e., if analytically extended, then for $r \to \infty$ it *does not decrease* as c/r (c is a constant) or faster.

This can be considered a *consequence of measurement errors.* The data given for $r = R_i$ are enough to determine a harmonic function in $\Omega_{ext} \equiv \{\boldsymbol{x} \in \boldsymbol{R}^3; r > R_i\}$ and thus in $\Omega \subset \Omega_{ext}$.

The data for $r = R_e$ have the nature of excess data and give rise to ("*internal*") *terms* $(r/R_e)^n T_n^{(e)}$ *not regular at infinity.*

Thus

$$T = T^{(i)} + T^{(e)}, \qquad T^{(i)} = \sum_{n=0}^{\infty} \left(\frac{R_i}{r}\right)^{n+1} T_n^{(i)}, \qquad T^{(e)} = \sum_{n=0}^{\infty} \left(\frac{r}{R_e}\right)^{n} T_n^{(e)}$$

***offers the general solution* in the domain Ω, *but* from the physical point of view its justification rests on a formal basis.**

Nevertheless **the term** $T^{(e)}$ **gives the possibility** ***to confront*** **the** ***two data sources considered*****. To see** ***an example*** **suppose that,**

$$T^{(EGM)} = \sum_{n=0}^{\infty} \left(\frac{R_i}{r} \right)^{n+1} T_n^{(EGM)}(\varphi, \lambda) \qquad \textbf{(9a)}$$

and

$$T^{(GOC)} = \sum_{n=0}^{\infty} \left(\frac{R_i}{r} \right)^{n+1} T_n^{(GOC)}(\varphi, \lambda) \qquad \textbf{(9b)}$$

are the disturbing potentials related to the ***EGM2008*** **and to the GOCE based** ***EGM-GOC-2*** **satellite-only model, respectively.**

Representing now**:**

$\Delta g(\varphi, \lambda) = \Sigma_{n=0}^{\infty} \Delta g_n(\varphi, \lambda)$ **in terms of** ***EGM2008*** **and**

$t(\varphi, \lambda) = \Sigma_{n=0}^{\infty} t_n(\varphi, \lambda)$ **in terms of** ***EGM-GOC-2*****, we know that**

$$\Delta g_n = \frac{n-1}{R_i} T_n^{(EGM)} \quad \textbf{and} \quad t_n = q^{n+1} T_n^{(GOC)}$$

Hence from Eq. (*4b*) we get that

$$T_n^{(e)} = c_n^{(p)} \left[T_n^{(GOC)} - T_n^{(EGM)} \right] \quad \text{with} \quad c_n^{(p)} = \frac{(n-1)\, q^{n+1}}{(n+2)(1+q^{2n+1}) - 3}$$

in case of *gravimetry and a satellite-only-model*.

Similarly, considering *gravimetry and gradiometry*, we get

$$T_n^{(e)} = c_n^{(g)} \left[T_n^{(GOC)} - T_n^{(EGM)} \right] \quad \text{with} \quad c_n^{(g)} = \frac{(n-1)(n+1)(n+2)\, q^{n+1}}{n(n-1)^2 + (n+1)(n+2)^2 q^{2n+1}}$$

The coefficients

$c_n^{(p)}$ **and** $c_n^{(g)}$

are illustrated on the right in *Figure 1*.

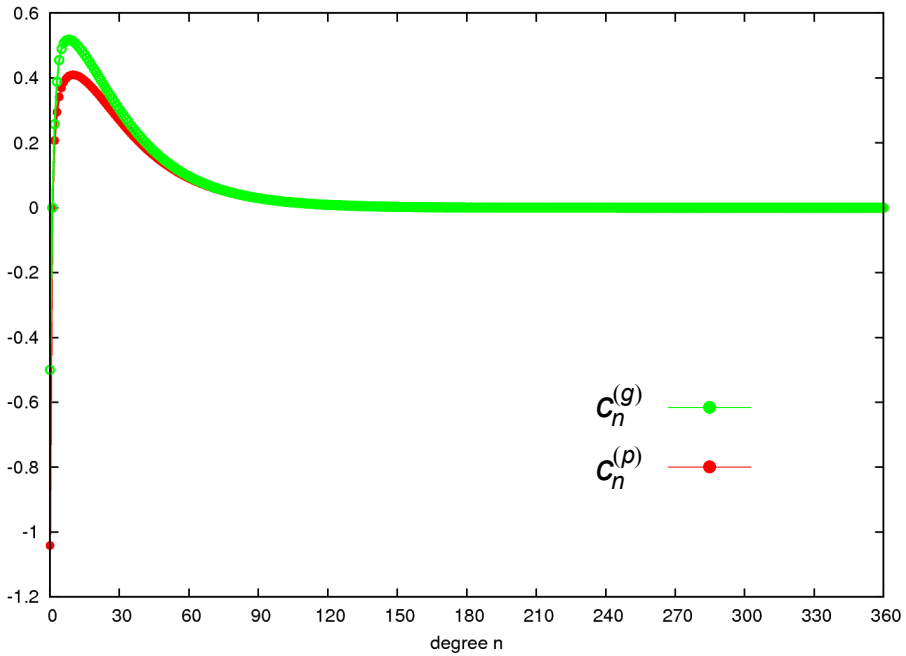

A better insight **offers a** ***plot of degree variances*** $\mathrm{var}\{T_n^{(e)}\}$ **.**
Recall, therefore, that

$$T_n^{(EGM)}(\varphi,\lambda)=\sum_{m=0}^{n}\left[\delta\bar{C}_{nm}^{(EGN)}\cos m\lambda+\delta\bar{S}_{nm}^{(EGN)}\sin m\lambda\right]\bar{P}_{nm}(\sin\varphi)$$

and

$$T_n^{(GOC)}(\varphi,\lambda)=\sum_{m=0}^{n}\left[\delta\bar{C}_{nm}^{(GOC)}\cos m\lambda+\delta\bar{S}_{nm}^{(GOC)}\sin m\lambda\right]\bar{P}_{nm}(\sin\varphi)$$

where, $\delta\bar{C}_{nm}^{(EGN)}$**,** $\delta\bar{S}_{nm}^{(EGN)}$ **and** $\delta\bar{C}_{nm}^{(GOC)}$**,** $\delta\bar{S}_{nm}^{(GOC)}$ **are coefficients of fully normalized surface spherical harmonics. Hence**

$$\mathrm{var}\left\{T_n^{(e)}\right\}=M\left\{\left[T_n^{(e)}\right]^2\right\}=$$

$$=\left[c_n^{(*)}\right]^2\sum_{m=0}^{n}\left\{\left[\delta\bar{C}_{nm}^{(GOC)}-\delta\bar{C}_{nm}^{(EGM)}\right]^2+\left[\delta\bar{S}_{nm}^{(GOC)}-\delta\bar{S}_{nm}^{(EGM)}\right]^2\right\}$$

Here M **stands for** ***the average over the whole unit sphere*****, while** $c_n^{(*)}$ **equals** $c_n^{(p)}$ **or** $c_n^{(g)}$ **in dependence of whether we consider our 1st or 2nd boundary value problem.**

The diagram computed for *EGM2008* and *EGM-GOC-2* is in *Figure 2* (*left*). (Note that for better illustration the *square root* of $\mathrm{var}\{T_n^{(e)}\}$ is plotted.)

***On the right of Figure 2* on can see the plot of the square root of $\mathrm{var}\{T_n^{(GOC)} - T_n^{(EGM)}\}$ for comparison.**

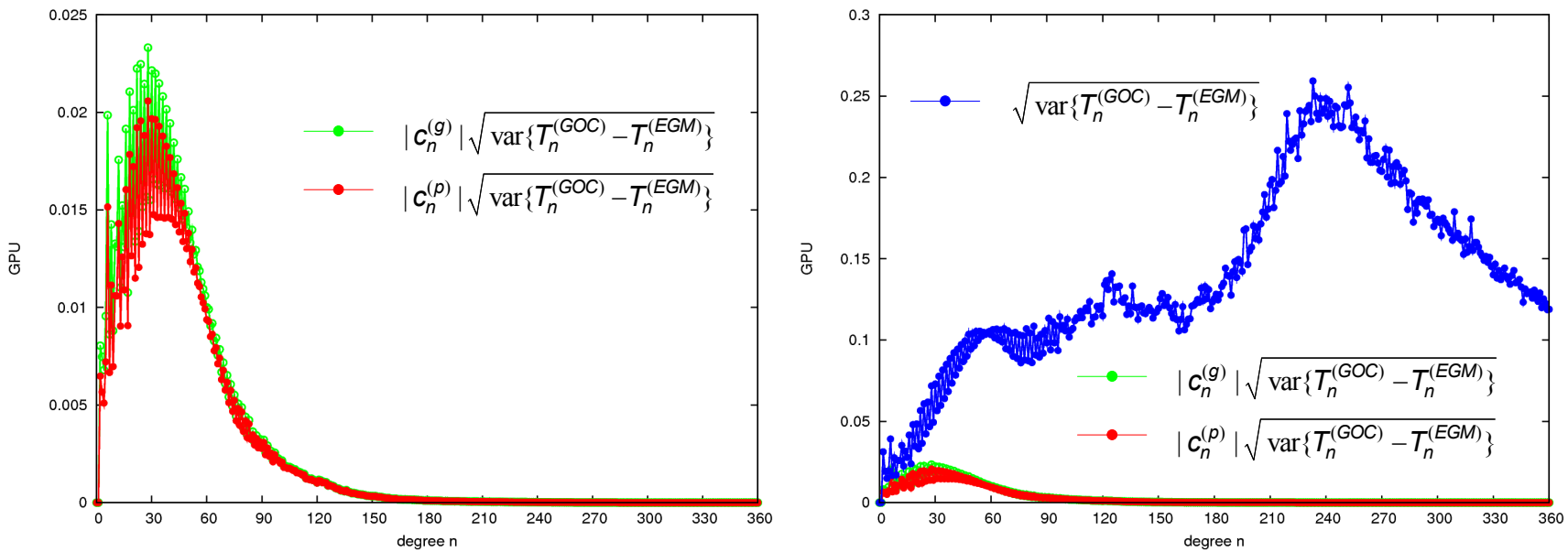

Figure 2. (*left*) The diagram of $\sqrt{\mathrm{var}\{T_n^{(e)}\}}$. (*right*) The diagram of $\sqrt{\mathrm{var}\{T_n^{(GOC)} - T_n^{(EGM)}\}}$.

***We also add* a global chart of $T^{(e)}$ and of $T_n^{(GOC)} - T_n^{(EGM)}$ for our 1st problem (*gravimetry and a satellite-only-model*).**

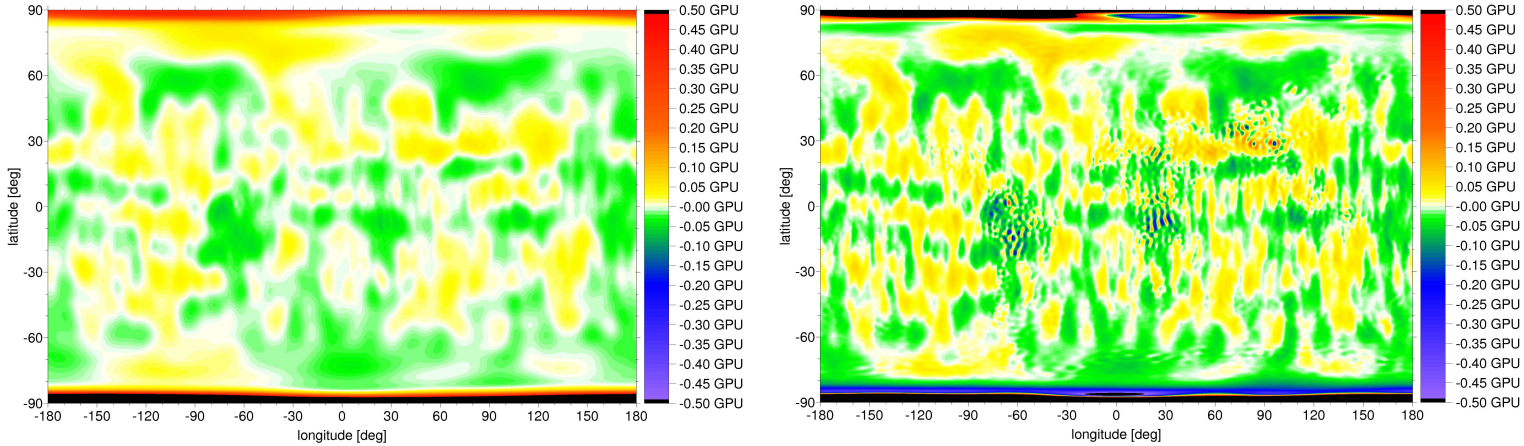

Figure 3. $T^{(e)}$ **for** $r = R_i$ **(*left*) and for** $r = R_e$ **(*right*).**

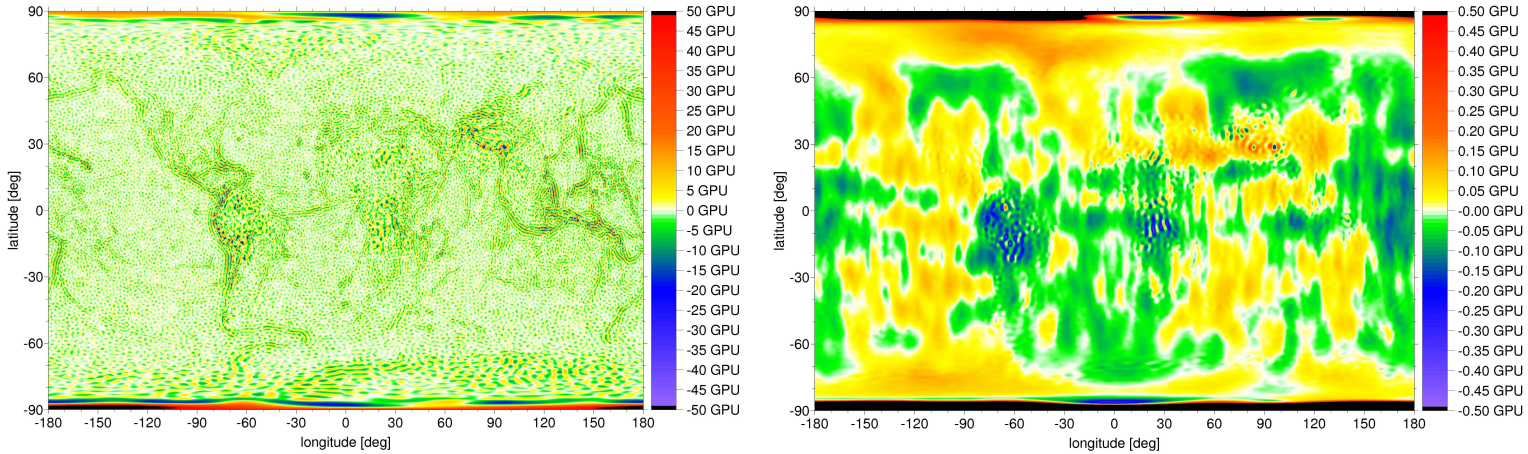

Figure 4. $T_n^{(GOC)} - T_n^{(EGM)}$ **for** $r = R_i$ **(*left*) and for** $r = R_e$ **(*right*).**

25. Optimization

In solving the incompatibility (*overdetermined problems*) *above*, we will look for a harmonic function f, regular at infinity that *minimizes the functional*

$$\Phi(f) = \int_{\Omega} (f - T)^2 \, d\boldsymbol{x}$$

We suppose that $f \in H_2(\Omega_{ext})$, where $H_2(\Omega_{ext})$ is a space of harmonic functions with inner product

$$(f, g) \equiv \int_{\Omega_{ext}} \frac{1}{r^2} fg \, d\boldsymbol{x}$$

The functional Φ attains its minimum in $H_2(\Omega_{ext})$. Hence, assuming Φ has its minimum at a point $f \in H_2(\Omega_{ext})$, its *Gâteaux' differentials equals zero* at f. This yields

$$\int_{\Omega} fv \, d\boldsymbol{x} = \int_{\Omega} Tv \, d\boldsymbol{x} \qquad \textbf{(18)}$$

for all $v \in H_2(\Omega_{ext})$.

Eq. (18) **represents** ***Euler's necessary condition*** **for** Φ **to have a minimum at** f**. It is a** ***starting point for a numerical solution.***

We put $v_{nm} = (R_i / r)^{n+1} Y_{nm}(\varphi, \lambda)$**, denoting by** Y_{nm} ***Laplace' surface spherical harmonics.***

Subsequently, $f = \Sigma_{n=0}^{\infty} \Sigma_{m=-n}^{m=n} f_{nm} v_{nm}$**, while** f_{nm} **are scalar coefficients. After some algebra we then easily obtain**

$$f = \sum_{n=0}^{\infty} \left(\frac{R_i}{r} \right)^{n+1} \left[T_n^{(i)} + \alpha_n T_n^{(e)} \right] \quad \text{with} \quad \alpha_n = \frac{(2n-1)(1-q^2)}{2(1-q^{2n-1})} q^{n-2} \qquad \textbf{(19)}$$

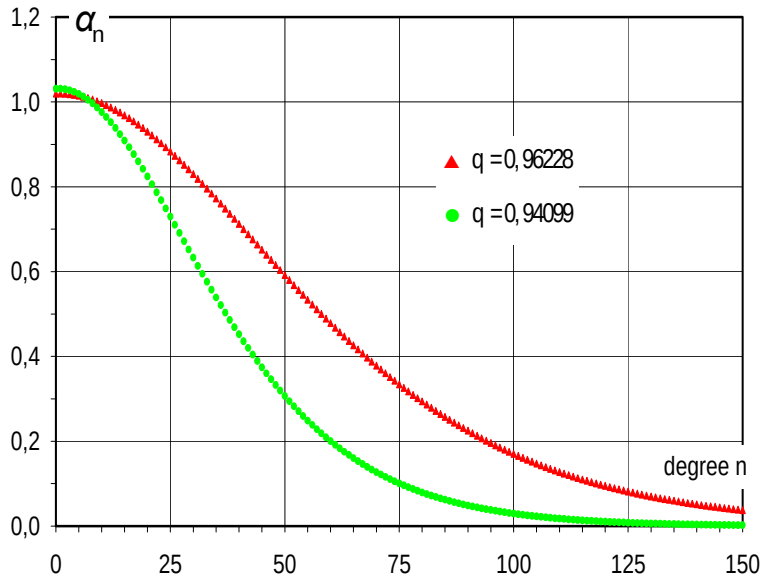

Figure 5. Values of α_n **for** $R_i = 6378\ km$ **and two cases of** R_e **:** $R_e = R_i + 250\ km$ **and** $R_e = R_i + 400\ km$**, i.e., for** $q = 0.96228$ **and** $q = 0.94099$**, respectively.**

Clearly, the optimized solution f is partially generated by $T_n^{(e)}$, but in contrast to *Eq.* (*3*), the influence of $T_n^{(e)}$ is modified by the factor α_n. This is illustrated in *Figure 6*. (*It is interesting to compare both the diagrams with* *Figure 2*.)

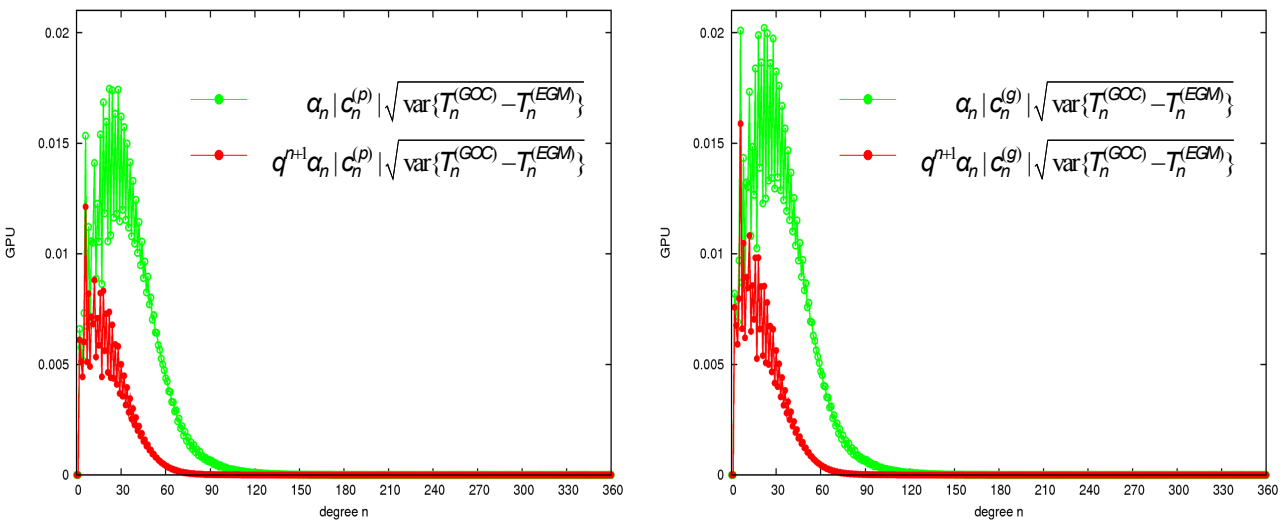

Figure 6. The diagrams of:

$$\sqrt{\mathrm{var}\{\alpha_n T_n^{(e)}\}} \text{ and } \sqrt{\mathrm{var}\{q^{n+1}\alpha_n T_n^{(e)}\}}$$

in case of the 1st problem (*left*) and the 2nd problem (*right*).

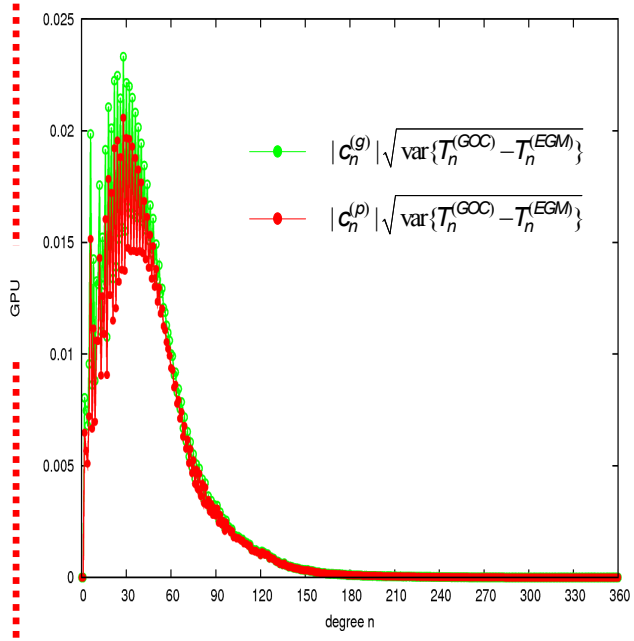

Figure 2.

(For comparison)

26. Optimized Solution – Influence of Input Data

To see the influence of the input data Δg, t and G on the optimized solution f we have to return to the original structure of the harmonics $T_n^{(i)}$ and $T_n^{(e)}$.

In particular, for the 1st problem (*gravimetry and a satellite-only model*) we obtain

$$f = \sum_{n=0}^{\infty} \left(\frac{R_i}{r} \right)^{n+1} \left[A_n^{(i)} \frac{R_i}{n-1} \Delta g_n + A_n^{(e)} t_n \right] \qquad \textbf{(20)}$$

with

$$A_n^{(i)} = \frac{(n-1)(1-\alpha_n q^{n+1})}{D_n^{(p)}} \quad \textbf{and} \quad A_n^{(e)} = \frac{(n+2)q^n + \alpha_n (n-1)}{D_n^{(p)}} \qquad \textbf{(21)}$$

where

$$D_n^{(p)} = (n+2)(1+q^{2n+1}) - 3$$

The values of the coefficients $A_n^{(i)}$ and $A_n^{(e)}$ are in *Figure 7* (*left*) that will follow

Similarly, for the 2nd problem (*gravimetry and gradiometry*) we have

$$f = \sum_{n=0}^{\infty} \left(\frac{R_i}{r} \right)^{n+1} \left[A_n^{(i)} \frac{R_i}{n-1} \Delta g_n + A_n^{(e)} \frac{R_e^2}{(n+1)(n+2)} G_n \right] \qquad \textbf{(22)}$$

with

$$A_n^{(i)} = (n-1)\left[n(n-1) - \alpha_n (n+1)(n+2) q^{n+1} \right] \frac{1}{D_n^{(g)}} \qquad \textbf{(23)}$$

$$A_n^{(e)} = (n+1)(n+2)\left[(n+2) q^n + \alpha_n (n-1) \right] \frac{1}{D_n^{(g)}} \qquad \textbf{(24)}$$

where $$D_n^{(g)} = n(n-1)^2 + (n+1)(n+2)^2 q^{2n+1}$$

The coefficients $A_n^{(i)}$ and $A_n^{(e)}$ are illustrated by *Figure 7* (*right*).

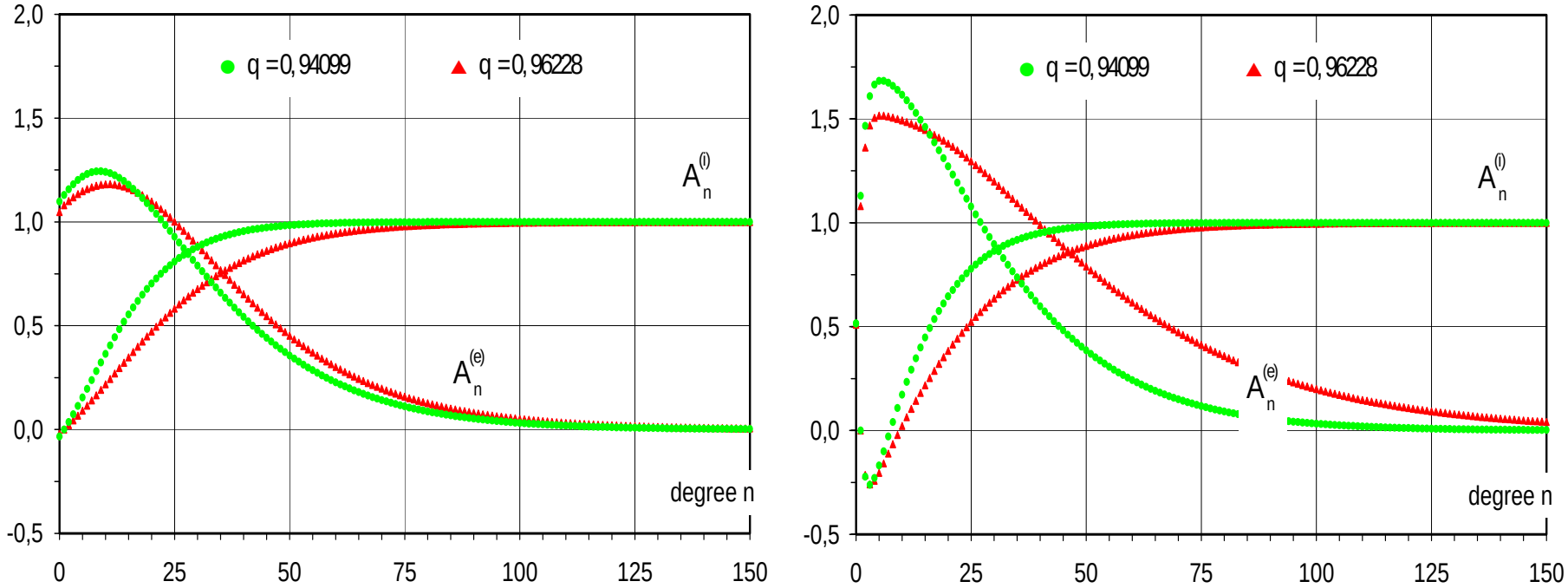

Figure 7. The coefficients $A_n^{(i)}$ and $A_n^{(e)}$ for $q = 0.96228$ and $q = 0.94099$ ($R_e = R_i + 250\ km$ and $R_e = R_i + 400\ km$) in case of (*left*) *gravimetry and a satellite-only model* and (*right*) *gravimetry and gradiometry*.

27. Terrestrial Term and the Integral Kernel

Recall that we obtained the following results (*optimized solution*):

- *1st problem* (*gravimetry and a satellite-only model*)

$$f = \sum_{n=0}^{\infty} \left(\frac{R_i}{r} \right)^{n+1} \left[A_n^{(i)} \frac{R_i}{n-1} \Delta g_n + A_n^{(e)} t_n \right]$$

- *2nd problem* (*gravimetry and gradiometry*)

$$f = \sum_{n=0}^{\infty} \left(\frac{R_i}{r} \right)^{n+1} \left[A_n^{(i)} \frac{R_i}{n-1} \Delta g_n + A_n^{(e)} \frac{R_e^2}{(n+1)(n+2)} G_n \right]$$

***Our aim is* to sum the series**

$$f_{terr} = \sum_{n=0}^{\infty} \left(\frac{R_i}{r} \right)^{n+1} A_n^{(i)} \frac{R_i}{n-1} \Delta g_n$$

representing the *terrestrial term* for the respective $A_n^{(i)}$.

For the *1st problem*, we get

$$f_{terr} = -\frac{R_i^2}{r} \cdot \frac{1-q}{2(2q-1)} \Delta g_0 + \frac{R_i^3}{r^2} \cdot \frac{2-(1+q)q}{6q^2} \Delta g_1 + \frac{R_i}{4\pi} \int_\sigma S^*(r,\psi) \Delta g \, d\sigma$$

with

$$S^*(r,\psi) = \sum_{n=2}^{\infty} A_n^{(i)} \frac{2n+1}{n-1} \left(\frac{R_i}{r} \right)^{n+1} P_n(\cos\psi)$$

While, for the *2nd problem* we obtain

$$f_{terr} = \frac{R_i^2}{r} \cdot \frac{1+q}{4q} \Delta g_0 - \frac{R_i^3}{r^2} \cdot \frac{1+q}{6q^2} \Delta g_1 + \frac{R_i}{4\pi} \int_\sigma S^*(r,\psi) \Delta g \, d\sigma$$

where $S^*(r,\psi)$ *appears again*, but with another coefficients $A_n^{(i)}$.

For $r = R_i$ the following figures shows *how the kernel* $S^*(r,\psi)$ *depends on the angle* ψ .

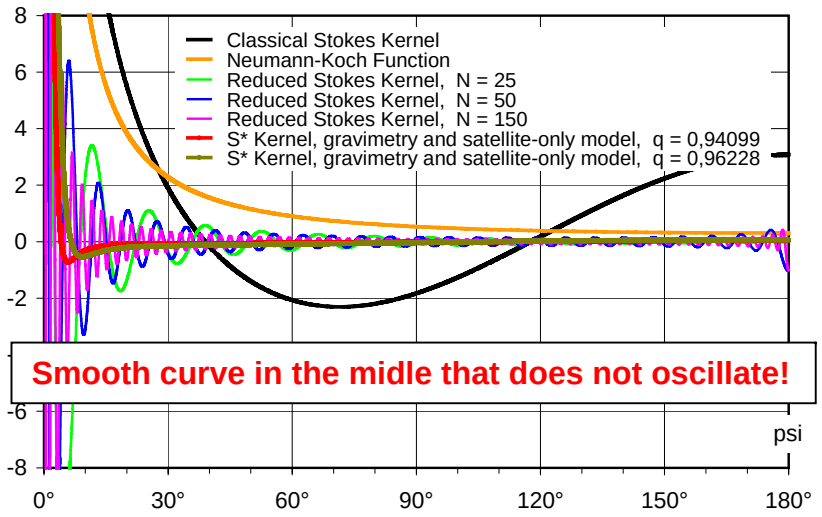

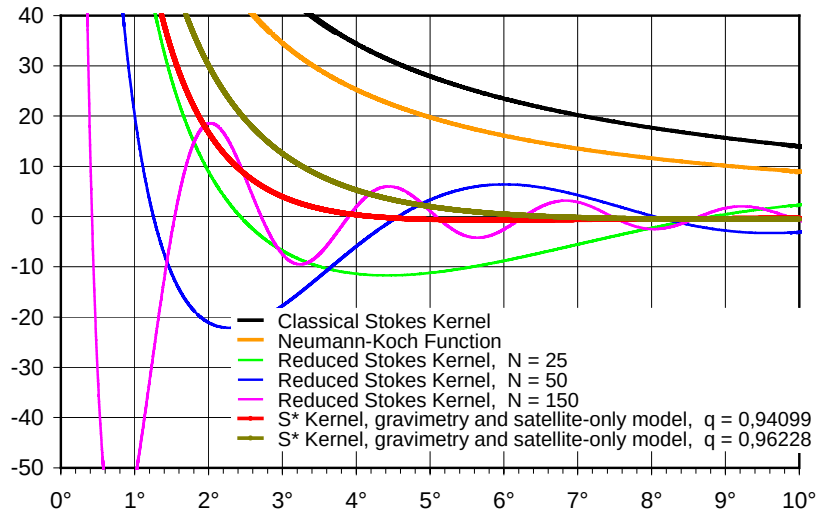

Note that very similar results **and figures can be obtained when using the *gravity disturbance*** δg **. In this case we have**

$$f = \sum_{n=0}^{\infty} \left(\frac{R_i}{r} \right)^{n+1} \left[A_n^{(i)} \frac{R_i}{n+1} \delta g_n + A_n^{(e)} t_n \right]$$ **with**

$$A_n^{(i)} = \frac{(n+1)(1-\alpha_n q^{n+1})}{D_n}$$ **and** $$A_n^{(e)} = \frac{n\, q^n + \alpha_n (n+1)}{D_n}$$

where $$D_n = 1 + n(1 + q^{2n+1})$$

The term

$$f_{terr} = \sum_{n=0}^{\infty} \left(\frac{R_i}{r} \right)^{n+1} A_n^{(i)} \frac{R_i}{n+1} \delta g_n$$

may then be represented by

$$f_{terr} = \frac{R_i}{4\pi} \int_{\sigma} K^*(r,\psi)\, \delta g \, d\sigma$$

with

$$K^*(r,\psi) = \sum_{n=2}^{\infty} A_n^{(i)} \frac{2n+1}{n+1} \left(\frac{R_i}{r} \right)^{n+1} P_n(\cos\psi)$$

Its dominant part (with respect to EGM2008) computed for *data from the territory of the Czech Republic* is plotted in the following *Figure 8*.

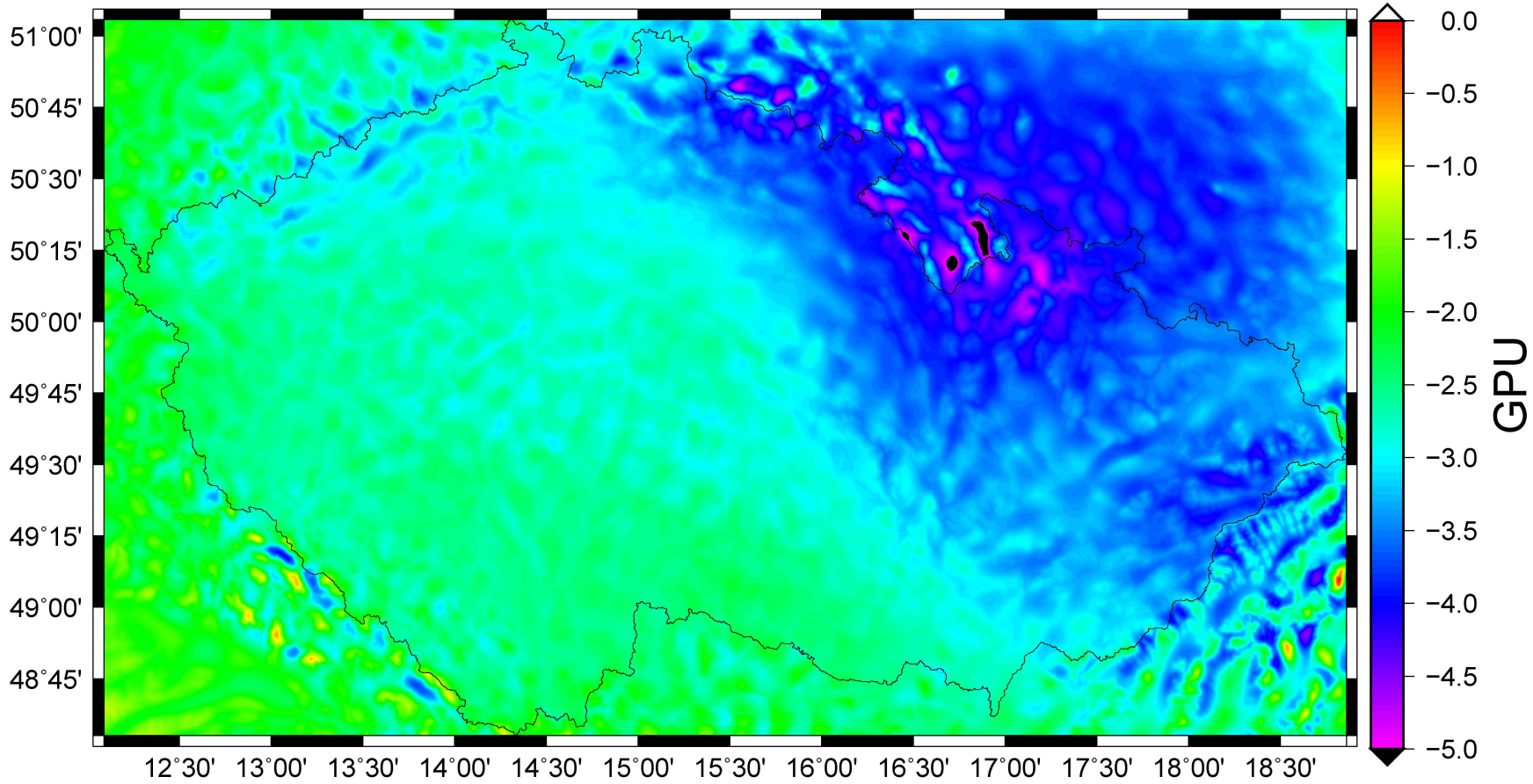

Figure 8

The composition $f = f_{terr} + f_{sat}$ **(where** $f_{sat} = \sum_{n=0}^{\infty} \left(\frac{R_i}{r} \right)^{n+1} A_n^{(e)} t_n$ **)**

is then in *Figure 9* .

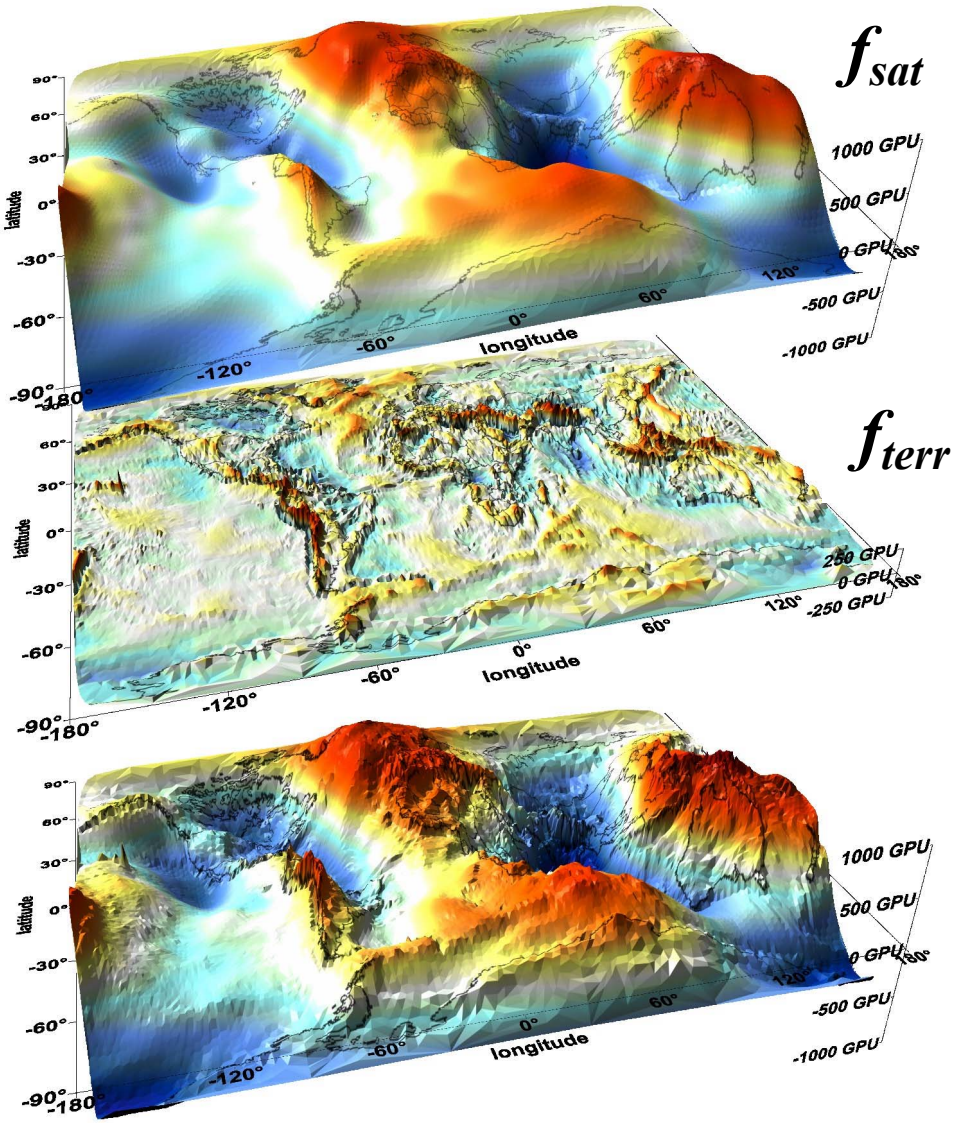

Figure 9. The composition $f = f_{terr} + f_{sat}$ **for** $r = R_i = 6378\ km$ **and** $q = 0.96228$ **(i.e.,** $R_e = R_i + 250\ km$ **).**
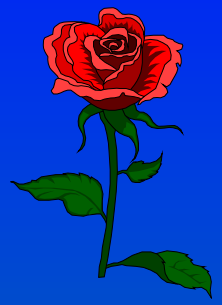
Thank you
for your attention !